Zeitschrift: IABSE reports = Rapports AIPC = IVBH Berichte

Band: 57/1/57/2 (1989)

Rubrik: Presentation Session 2a: Durability of reinforced concrete: concrete deterioration

PRESENTATIONS

Leere Seite
Blank page
Page vide

Diffusion de gaz et durabilité du béton armé

Gasdiffusion und Dauerhaftigkeit von Stahlbeton

Diffusion of Gas and Durability of Reinforced Concrete

Yves F. HOUST
Chimiste
Ecole Polytechnique Fédérale
Lausanne, Suisse

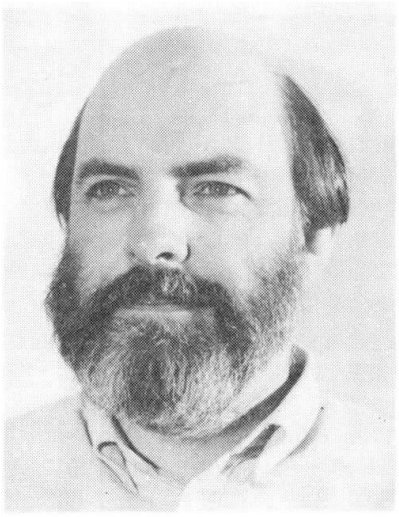

Yves F. Houst, né en 1946, est diplômé de chimie de l'Université de Lausanne. Il travaille dans le domaine des matériaux de construction depuis 16 ans. Il est actuellement chef de la section chimie au Laboratoire des Matériaux de Construction de l'Ecole Polytechnique Fédérale de Lausanne.

Folker H. WITTMANN
Professeur
Ecole Polytechnique Fédérale
Zurich, Suisse

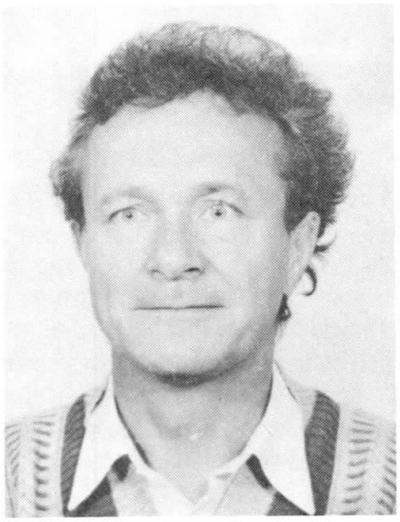

Folker H. Wittmann, né en 1936, est gradué en physique. Il fut 4 ans professeur de matériaux de construction à l'Université technique de Delft (Pays-Bas) et 8 ans à l'Ecole Polytechnique Fédérale de Lausanne. Il est actuellement Professeur ordinaire de matériaux de construction à l'Ecole Polytechnique Fédérale de Zurich.

RÉSUMÉ

Une méthode de mesure du coefficient de diffusion des gaz à travers la pâte de ciment durcie est décrite. On peut surtout étudier l'influence de la teneur en eau et de la porosité sur la diffusion de l'oxygène et du gaz carbonique. Les premiers résultats sont indiqués.

ZUSAMMENFASSUNG

Es wird eine Methode zur Bestimmung der Gasdiffusionskoeffizienten von Zementstein beschrieben. Insbesondere der Einfluss des Feuchtigkeitsgehaltes und der Porosität auf die Diffusion von Sauerstoff und Kohlendioxid kann damit untersucht werden. Über erste Ergebnisse wird berichtet.

SUMMARY

A method to determine the coefficients of gas diffusion in hardened cement paste is described. The influence of moisture content and porosity on diffusion of oxygen and carbon dioxide in particular can be studied. Preliminary results are presented.

1. INTRODUCTION

La carbonatation du béton armé et ses conséquences sur la corrosion des armatures est un phénomène connu depuis longtemps. A titre d'exemple, on peut citer un article de B. Zschokke datant de 1916 [1] qui décrit déjà les causes de carbonatation du béton, la corrosion des armatures et les précautions à prendre pour limiter les dégâts. Jusqu'au moins au début des années soixante, les problèmes liés à la carbonatation du béton et à la corrosion des armatures n'ont que peu touché les ingénieurs constructeurs qui se sont plutôt concentrés sur de nouvelles méthodes de construction. Toutefois, ces deux dernières décennies, l'augmentation très rapide des dégâts, le coût des réparations et de l'entretien [2, 3] ont crû de telle façon que de nombreuses personnes ont commencé à s'occuper du comportement à long terme du béton armé et précontraint.

De nombreuses publications traitent de la carbonatation. Récemment, Parrott [4] a compilé une bibliographie sur la carbonatation du béton armé et recensé 182 articles datant essentiellement des vingt dernières années. Cependant, tous ces efforts ont certainement permis de mieux comprendre le phénomène de la carbonatation et les facteurs qui l'influencent, mais par contre les méthodes de prévision de la durée de vie des constructions nouvelles ou existantes ne sont actuellement pas fiables. Ainsi, il n'est pas possible de concevoir, entretenir ou réparer les structures avec toute l'efficacité souhaitable. Cette situation exige une recherche détaillée des différents processus impliqués.

Jusqu'à maintenant, l'essentiel des recherches a porté sur l'étude phénoménologique et empirique de parties d'un problème très complexe. Les méthodes traditionnelles ne permettent pas de faire la synthèse de toutes les connaissances acquises et de développer ainsi des méthodes capables de prévoir la durée de vie des structures de façon réaliste. Le développement de nouvelles méthodes devrait permettre de décrire quantitativement les effets de l'humidité, de la teneur en dioxyde de carbone, de la température, des chlorures, de la cure, du type de ciment, de la composition du béton, de revêtements protecteurs sur la carbonatation et la vitesse de corrosion de l'acier d'armature.

Actuellement, la simulation numérique permet de traiter quantitativement des processus interactifs complexes. C'est ce que nous allons tenter de montrer dans cet article, en décrivant brièvement quelques modèles. On montrera également qu'il est nécessaire d'étudier certaines propriétés des matériaux et donnera à titre d'exemple, la mesure du coefficient de diffusion de l'oxygène et du dioxyde de carbone à travers des pâtes de ciment en fonction de l'humidité.

2. EFFETS DE LA CARBONATATION SUR LA DURABILITE DU BETON ARME

La carbonatation du ciment est la réaction de neutralisation de ses composés basiques sur le dioxyde de carbone ou gaz carbonique présent dans l'air. Cette réaction atteint tous les composés hydratés à l'exception du gypse. Dans certaines conditions, même les composés anhydres peuvent réagir. Du point de vue pratique, ce sont essentiellement l'hydroxyde de calcium, $Ca(OH)_2$, et les silicates de calcium hydratés qui jouent un rôle important. La carbonatation de ces derniers composés conduit à la formation de carbonate de calcium ($CaCO_3$), de silice (SiO_2) et d'eau. Les mécanismes chimiques sont décrits plus en détail dans une autre communication à ce même symposium [5]. La carbonatation dépend d'un grand nombre de paramètres. Les influences les plus importantes sont décrites dans la publication de Parrott déjà mentionnée [2].

On trouve dans la littérature deux concepts de base qui décrivent mathématiquement l'avancement du processus de carbonatation. La plus ancienne théorie est basée sur une loi en $\sqrt{t}$ qui est une solution de l'équation de diffusion. Les valeurs empiriques montrent toutefois que l'exposant du temps est un peu inférieur à 0.5 et diminue légèrement pour de longues durées. Schiessl [6] a introduit un facteur de retardement qui conduit à un maximum de profondeur de carbonatation fini pour $t = \infty$. Cette conclusion ne peut être absolument correcte. Cette approche peut toutefois être réaliste pour des durées de vie des constructions de 80 à 100 ans.

Lorsque le béton directement en contact avec les armatures se carbonate, l'eau des pores subit une forte baisse du pH. Dans ces conditions nouvelles, l'acier ne bénéficie plus de la protection que lui assurait un pH élevé. Dans certaines conditions, notamment avec une humidité relativement élevée, l'acier peut se corroder

à une vitesse qui dépend de nombreux paramètres [7]. Il faut en particulier avoir à disposition suffisamment d'oxygène qui doit également diffuser depuis la surface du béton en contact avec l'atmosphère. La présence de chlorures, provenant essentiellement des sels de déverglaçage ou d'adjuvants, supprime la protection dont bénéficie l'acier dans un milieu à pH élevé.

3. MODELISATION

La modélisation de problèmes de durabilité a été étudiée au Laboratoire des Matériaux de Construction (LMC) de l'Ecole Polytechnique Fédérale de Lausanne (EPFL) selon plusieurs approches. Denarié [8] a montré comment développer une méthode tenant compte des incertitudes inhérentes au phénomène (approche probabiliste) qui permet d'évaluer l'état présent d'une construction et de calculer sa durée de vie probable. Un processus stochastique a été utilisé pour évaluer la distribution de la profondeur de carbonatation dans le temps et une distribution normale pour la couverture des armatures. La comparaison des résultats obtenus par le calcul de la probabilité de défaillance, à partir des distributions de valeurs théoriques et mesurées, montre le bien fondé des approximations faites. Enfin, cet auteur propose d'utiliser un système expert de diagnostic et d'analyse pour reprendre la démarche effectuée afin de fournir de véritables outils d'étude d'ouvrages endommagés.

Dans une première étude, Brieger et Wittmann [9] ont décrit le processus de carbonatation au moyen d'un système d'équations aux dérivées partielles, qui leur ont permis d'étudier les facteurs les plus importants, ainsi que divers mécanismes. La résolution des équations a été effectuée par voie numérique. Une autre approche a été faite par Brieger et Bonomi [10] qui ont été inspirés de modèles de la dynamique des fluides pour construire un modèle discret en temps et en espace d'automate cellulaire probabiliste. Cette méthode laisse entrevoir d'intéressants développements.

Dans une première tentative, Houst et al. [11] ont tenté d'étudier la carbonatation au moyen d'un modèle numérique. Tous les paramètres utilisés peuvent être reliés à des propriétés mesurables qui sont définies pour une composition du béton et un environnement donnés. Cet exemple nous paraît intéressant, car il permet clairement de montrer le genre de paramètre à déterminer expérimentalement.

Les équations (1), (2) et (3) suivantes permettent d'étudier l'interaction mutuelle du séchage et de la diffusion du dioxyde de carbone sur la carbonatation.

Le béton jeune peut être considéré comme un matériau poreux saturé d'eau. Le séchage peut être décrit par une équation de diffusion. Pour un tel béton, la carbonatation se superpose au séchage. Pendant ce processus de l'eau est libérée dans le béton. Il faut donc ajouter un terme à l'équation de diffusion pour tenir compte de la libération d'eau :

$$\frac{\partial w}{\partial t} = \frac{\partial}{\partial x} D_w \frac{\partial w}{\partial x} + \alpha_1 \frac{\partial c}{\partial t} \qquad (1)$$

Dans cette équation, w représente l'eau évaporable et D_w le coefficient de diffusion de vapeur d'eau. Ce coefficient dépend de la teneur en eau. c représente la quantité de carbonate formé et α_1 est un paramètre du matériau qui tient compte du dosage en ciment et du rapport e/c. Dans l'étape suivante, il faut décrire la pénétration du dioxyde de carbone dans le système poreux du béton. En première approximation, on peut à nouveau utiliser l'équation générale de la diffusion. La réaction de carbonatation consomme du dioxyde de carbone. En tenant compte de cette perte, on peut écrire l'équation différentielle (2) suivante :

$$\frac{\partial g}{\partial t} = \frac{\partial}{\partial x} D_g \frac{\partial g}{\partial x} - \alpha_2 \frac{\partial c}{\partial t} \qquad (2)$$

Dans cette équation, D_g est le coefficient de diffusion du CO_2. Il dépend de la teneur en humidité. α_2 est à nouveau un paramètre du matériau qui dépend essentiellement de la composition du béton.

La vitesse de carbonatation dépend du degré de carbonatation, de la concentration en CO_2 et finalement de la teneur en eau du béton. En admettant que l'on puisse combiner ces trois influences majeures sous forme de facteurs, on obtient :

$$\frac{\partial c}{\partial t} = \alpha_3 \cdot f_1(c) \cdot f_2(g) \cdot f_3(w) \qquad (3)$$

α_3 est à nouveau un paramètre du matériau qui tient compte de la composition du béton et du degré d'hydratation. Un développement plus détaillé de ce modèle est donné dans [11].

En résolvant les équations (1), (2) et (3) on peut étudier l'interaction mutuelle du séchage et de la diffusion du CO_2 sur la carbonatation. Un modèle numérique basé sur ces trois équations a été développé et la méthode des différences finies utilisée pour résoudre les équations du modèle numérique.

Actuellement, les valeurs des paramètres du modèle sont loin d'être toutes connues. L'étude de ces paramètres peut être relativement complexe, comme l'exemple donné dans la partie suivante nous le montre.

Toutefois, soit à l'aide de valeurs de paramètres tirées de la littérature, soit estimées, une solution numérique du système de trois équations différentielles donné précédemment, a permis de déterminer la profondeur de carbonatation de deux types de béton en fonction du temps. Les résultats obtenus à l'aide du modèle montrent qu'après une carbonatation initiale rapide, l'avancement de la carbonatation suit approximativement une loi en $\sqrt{t}$. Ces résultats, comparés à des mesures effectuées in situ, se sont avérés tout à fait réalistes.

4. MESURE DE LA DIFFUSION D'UN GAZ

4.1. Préparation des échantillons

Afin de déterminer le coefficient de diffusion D_g du modèle décrit ci-dessus, nous avons été amené à préparer des échantillons qui devaient être suffisamment minces pour pouvoir être complètement carbonatés et équilibrés à différentes humidités relatives dans un temps relativement court. Pour cela, nous avons confectionné des cylindres de pâte de ciment de diamètre 160 mm qui après au moins six mois de cure dans l'eau ont été coupés en disques de 1 à 2 mm d'épaisseur. Comme il n'est pas possible de varier le rapport eau/ciment de pâtes de ciment de façon notable sans avoir de décantation, nous avons dû maintenir les grains de ciment en suspension en faisant tourner le cylindre jusqu'à ce que la prise évite toute décantation, ce qui nous a permis de varier le rapport e/c entre 0.3 et 0.8. Pour cela, nous nous sommes inspirés de la méthode décrite par Sereda et Swenson [12], mais nous avons dû y apporter certaines modifications étant donné le grand diamètre de nos échantillons par rapport à ceux de Sereda et Swenson (Ø 32 mm). Lors de la carbonatation naturelle le gaz diffuse dans un matériau carbonaté. Nous avons donc carbonaté artificiellement nos échantillons et les avons équilibrés dans le climat correspondant à l'h.r. à laquelle nous effectuons la mesure.

4.2. Mesure des coefficients de diffusion de O_2 et CO_2

Comme la disponibilité d'oxygène à proximité de l'armature susceptible de se corroder est un facteur important et que la mesure de la diffusion d'oxygène n'entraînait pas de complication particulière, nous avons développé un système de mesure. Le coeur de ce système est une cellule de mesure séparée en deux chambres par le disque du matériau à tester. Avant les mesures, on purge les deux chambres avec de l'azote pur contenant la quantité de vapeur d'eau nécessaire à l'obtention de l'h.r. désirée. Au début de la mesure, on fait pénétrer dans la chambre supérieure un mélange de gaz artificiel (78% N_2, 20% O_2, 2% CO_2) dont l'h.r. est la même que celle de l'azote utilisé pour la purge du système. Ce gaz est régulièrement renouvelé dans la chambre supérieure où la concentration des différentes espèces est constante peu après le début des mesures. Au cours du temps, on analyse la concentration en O_2 et CO_2 dans la chambre inférieure par un analyseur en circuit fermé. Dans cette chambre, la concentration en O_2 varie donc de 0 à 20 % et celle en CO_2 de 0 à 2 %. Les coefficients de diffusion de O_2 et CO_2 peuvent être calculés à partir

des courbes de concentration de ces gaz en fonction du temps. Le système a d'abord été testé avec du béton cellulaire autoclavé. Les résultats obtenus, ainsi qu'une description plus détaillée du système de mesure figurent dans [13].

5. RESULTATS ET DISCUSSION

La diffusion des deux gaz a été mesurée à travers des échantillons équilibrés à deux différentes h.r. Les résultats sont donnés dans la table. Les valeurs moyennes et l'écart type y sont indiqués. Le nombre de mesures individuelles est donné par n. Toutes les valeurs sont reprises dans la figure.

Comme on pouvait s'y attendre le coefficient de diffusion augmente sensiblement avec le rapport eau/ciment. Dans le domaine de nos mesures le coefficient de diffusion ne dépend pas de la teneur en eau. Des mesures à des h.r. plus élevées sont maintenant en route. On peut s'attendre à ce que le coefficient de diffusion diminue lorsque les capillaires de la pâte de ciment durcie se remplissent progressivement d'eau.

	e/c = 0.4		e/c = 0.8	
Humidité relative	D_{O2} [$cm^2 \cdot s^{-1}$]	D_{CO2} [$cm^2 \cdot s^{-1}$]	D_{O2} [$cm^2 \cdot s^{-1}$]	D_{CO2} [$cm^2 \cdot s^{-1}$]
48 %	$(7.6 \pm 2.1) \cdot 10^{-5}$ (n = 4)	$(5.8 \pm 2.1) \cdot 10^{-5}$ (n = 4)	$(1.8 \pm 0.5) \cdot 10^{-3}$ (n = 8)	$(1.4 \pm 0.5) \cdot 10^{-3}$ (n = 8)
55 %	$(7.7 \pm 1.9) \cdot 10^{-5}$ (n = 7)	$(5.6 \pm 1.6) \cdot 10^{-5}$ (n = 7)	$(2.1 \pm 0.6) \cdot 10^{-3}$ (n = 6)	$(1.6 \pm 0.5) \cdot 10^{-3}$ (n = 6)

Table : Coefficient de diffusion D de O_2 et CO_2 mesuré sur deux pâtes de ciment (e/c: rapport eau/ciment lors du gâchage, n= nombre de mesures).

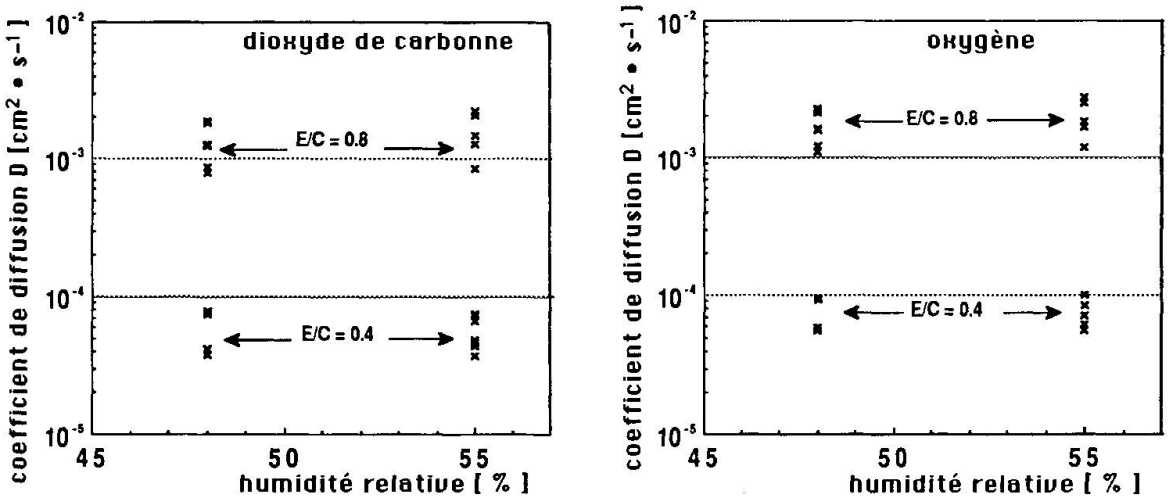

Fig. Coefficients de diffusion de CO2 et O2 dans la pâte de ciment durcie mesurés à 48 et 55 %.

6. CONCLUSIONS

Nous avons développé une méthode qui nous permet de déterminer le coefficient de diffusion du gaz carbonique et de l'oxygène dans la pâte de ciment durcie en fonction de la teneur en eau.

Le coefficient de diffusion dépend fortement du rapport eau/ciment.

Dans le béton ce n'est que la pâte de ciment durcie qui subit la carbonatation. Il est pratiquement impossible cependant de mesurer les coefficients de diffusion directement sur des échantillons en béton. Il faut encore développer un modèle d'un matériau composite qui permette de transposer les résultats obtenus et décrits ici au béton.

BIBLIOGRAPHIE

1. ZSCHOKKE B., Über das Rosten der Eiseneinlagen im Eisenbeton, Schweiz. Bauzeitung, LXVII (1916) 285-289.
2. PARROTT L.J., A review of carbonation in reinforced concrete, Cement and Concrete Association, Wexham Springs (1987).
3. WITTMANN F.H., Structure et durabilité du béton armé in Durabilité du béton armé, documentation SIA 89, SIA, Zürich (1985) pp. 7-14.
4. PARROTT L.J., Carbonation in reinforced concrete: A bibliography, Cement and Concrete Association, Wexham Springs (1987).
5. HOUST Y.F. et WITTMANN F.H., Le retrait de carbonatation, communication à ce symposium.
6. SCHIESSL P., Zur Frage der zulässigen Rissbreite und der erforderlichen Betondeckung im Stahlbetonbau unter besonderer Berücksichtigung der Karbonatisierung des Betons, Deutscher Ausschuss für Stahlbeton, Heft 255, Wilhelm Ernst & Sohn, Berlin-München-Düsseldorf (1976).
7. SCHIESSL P., Korrosion der Bewehrung im Stahlbeton, Bausanierung und Bautenschutz, Sonderheft (1983) pp. 64-71.
8. DENARIE E., Carbonatation - Durée de vie de bâtiments en béton armé, Chantiers/Suisse, 19 (1988) 89-92 et 149-151.
9. BRIEGER L.M., WITTMANN F.H., Numerical simulation of carbonation of concrete, in (F.H. Wittmann Ed.), Material Science and Restoration, Technische Akademie Esslingen, Ostfildern (1986) 635-640.
10. BRIEGER L.M., and BONOMI E., A cellular automaton model of diffusion and reaction in a porous medium: Concrete, Supercomputing Review, november 1988, pp. 3-4.
11. HOUST Y.F., ROELFSTRA P.E., and WITTMANN F.H., A model to predict service life of concrete structures, in (F.H. Wittmann Ed.), Material Science and Restoration, Ed. Lack + Chemie, Filderstadt (1983) 181-186.
12. SEREDA P.J., and SWENSON E.G., Apparatus for preparing portland cement paste of high water-cement ratio, Mat. Res. & Standards, 7 (1967) 152-154.
13. HOUST Y.F., and WITTMANN F.H., The diffusion of carbon dioxide and oxygen in aerated concrete, in (F.H. WITTMANN Ed.) Materials Science and Restoration, Technische Akademie Esslingen, Ostfildern (1986) 629-634.

Evaluation of On-site Conditions and Durability of Concrete Panels Exposed to Weather

Prévision de la durabilité de parois en béton exposées aux intempéries

Vorhersage der Dauerhaftigkeit bewitterter Betonbauten

Ferdinand S. ROSTÁSY
Prof. Dr.-Ing.
TU Braunschweig
Braunschweig, FR Germany

F. S. Rostásy, born 1932, professor for structural materials, at the Institut für Baustoffe, Massivbau und Brandschutz.

Dieter BUNTE
Dipl.-Ing.
TU Braunschweig
Braunschweig, FR Germany

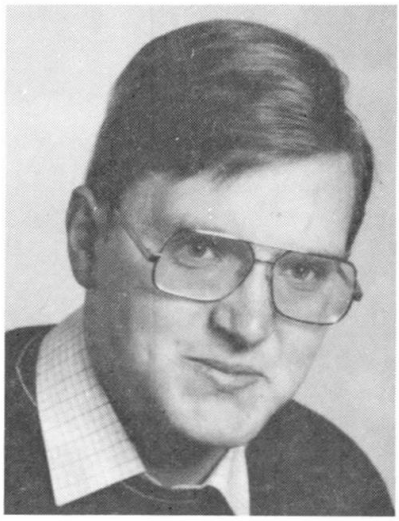

D. Bunte, born 1959, research assistant for structural materials, at the Institut für Baustoffe, Massivbau und Brandschutz.

SUMMARY

A model for the prediction of durability of concrete panels exposed to weather is developed. This model combines a carbonation law derived on basis of the reaction process with on-site non-destructive measurements of the permeability of cover.

RÉSUMÉ

Un modèle pour la prévision de la durabilité de parois en béton exposées aux intempéries est dévoloppé. Ce modèle lie une loi de la carbonatation avec des mesures de la perméabilité du béton d'enrobage.

ZUSAMMENFASSUNG

Zur Vorhersage der Dauerhaftigkeit von Stahlbetonbauten wird ein Modell entwickelt, das einen physikochemisch begründeten Ansatz der Karbonatisierungstiefenberechnung mit Ergebnissen von Dichtigkeitsmessungen am Bauwerk verknüpft.

1. INTRODUCTION

Durability is generally defined as the characteristic property which ensures function, structural safety and adequate appearance of a r/c-member during service life with a minimum of maintenance. For a specific case, however, durability must be defined in terms of environment and potential type of damage. The most common damage is the corrosion of the reinforcement near the surface of the r/c-member. In this case, durability may be regarded as exhausted as soon as peaks of the carbonation front with pH 9 reach - with a certain probability - regions of the steel with a minimum cover. Thus, durability is defined as incubation time of corrosion as a function of depth and tightness of cover. In this report a prediction model is presented which combines a physicochemical law of carbonation with the results of non-destructive on-site permeability tests.

2. MODEL FOR THE PREDICTION OF DURABILITY

2.1 Range of validity of model

The prediction model is valid for r/c-members exposed to normal weather of Central Europe and for essentially vertical surfaces. Concrete with a quality of C 25 to C 35 made with portland cement and frost-resistant natural aggregate is considered; complete compaction is presupposed. The model is valid for any type of curing. The model describes the carbonation progress in uncracked concrete. It is, however, also applicable for cracked r/c-members as long as the 95 %-fractile of the actual, measured crack widths does not exceed 0,25 to 0,30 mm.

2.2 Schießl's carbonation law

The progress of carbonation can be described with Schießl's law [1]. The mean final depth of carbonation is given by

$$\bar{x}_\infty = \frac{D_{co}}{\bar{b}} \Delta c \qquad (1)$$

with

Δc .... difference of CO_2-concentration of air between surface and carbonation front ($\approx 0{,}6^2$ g/m³ in urban and $\approx$ 0,8 - 1,0 g/m³ in polluted industrial areas, 0,54 g/m³ as average value).

D_{co} ... coefficient of CO_2-diffusion through carbonated concrete at the member's surface at the age of about 90 d and for the mean annual moisture content of concrete cover.

$\bar{b}$ ..... coefficient taking into account the realkalization of carbonated concrete by $Ca(OH)_2$-diffusion and the dependence of D_{co} on depth of carbonation, moisture of concrete, etc.

The progress of carbonation is described by:

$$t = -\frac{a}{\bar{b}}\left[x + x_\infty \ln\left(1 - \frac{x}{x_\infty}\right)\right] \qquad (2)$$

with a, content of all relevant alkaline hydration products which can be converted into carbonates.

The Equ.(1) and (2) were derived by idealization of the complex physicochemical reactions of carbonation. For prediction, representative values for the coefficient of Equ.(1) were proposed in [1]. Experiments show their wide range and considerable scatter. Thus, the prediction of durability of a specific structure solely on basis of representative values of D_{co}, $\bar{b}$ and Δc is insecure. Uncertainty can be reduced if the carbonation depth and D_{co} are measured. This, how-

ever, can only be performed in the laboratory, considerable core extraction becomes necessary. Because such procedure is usually impossible, the necessary information on the diffusivity for CO_2 must be acquired by substitutive on-site absorption tests such as ISA [2]. Such tests can be performed non-destructively and repeatedly.

2.3 Combination of carbonation law and ISA test results

By the ISA-test the absorption of water is measured as function of suction time t_s. The ISA-value is related to pore structure data of the first 10 to 20 mm of cover. These date incorporate the influence of compositional parameters of concrete, curing, carbonation, etc. Consequently, they also describe the diffusivity for CO_2 and water vapour. As explained and verified in [2], [3] the ISA-value can be expressed by:

$$ISA(t_s) = \frac{K_2 \sqrt{2r_h}\, \epsilon_{abs}}{2\rho_w a_{Tabs}}\, t_s^{-\frac{1}{2}} \tag{4}$$

Meaning of the parameters in Equ.(4) were defined in [2]. ϵ_{abs} is the effective porosity for absorption ($r \geq 100$ nm). The effective porosity for gas diffusion ϵ_{diff} exceeds ϵ_{abs} because pores with $r \geq 30$ nm become accessible. Tortuosity of diffusion consequently also increases. Acc. to [3], the following relations can be formulated:

$$\begin{aligned} \epsilon_{diff} &\approx 1{,}7\ \epsilon_{abs} \\ a_{Tdiff} &\approx 1{,}5\ a_{Tabs} \end{aligned} \tag{5}$$

The unknown coefficient D_C for CO_2-diffusion can be expressed by:

$$D_C = D_a \frac{\epsilon_{diff}}{a_{Tdiff}} \tag{6}$$

with D_a, the diffusivity of CO_2 through air (0,159 cm^2/s at 20 °C). By insertion of Equ.(4), (5), and (6) into Equ.(1), we obtain the prediction value of the mean, final carbonation depth based on the mean $ISA_{(10\ min.)}$-value:

$$\overline{x}_\infty \approx \frac{D_a \Delta c}{\overline{b}\, K_3} \frac{\overline{ISA}_{10}}{\sqrt{2r_h}} \tag{7}$$

Progress function follows Equ.(2). Fig. 1 shows the evaluation of Equ.(7) for several mean values of ISA_{10} vs. age.

3. APPLICATION

3.1 Variability and durability criterion

The prediction model Equ.(7) contains essentially the same assumptions as Equ.(1). Though, by on-site measurement a realistic assessment of diffusivity becomes possible, the other coefficients must still be chosen within a reasonable range. Thereby, their scatter is taken into account. Furthermore, the ISA-value depends on the moisture and temperature of concrete at test. The effect of the difference between the temperature at test and the mean annual temperature ($\overline{T} \approx 12$ °C) can be taken into account. ISA-tests have to be performed a certain drying time after rainfall. It is assumed, that the moisture of concrete at this state corresponds to the mean annual value. The unknown scatter of the constituents of Equ.(7) is globally satisfied by a coefficient of variation of ≈ 40 % of carbonation depth [1]. Thus, we obtain for the 95 %-fractile of the carbonation depth at any age t:

$$x_{95}(t) \approx 1{,}7\ \overline{x}(t) \tag{8}$$

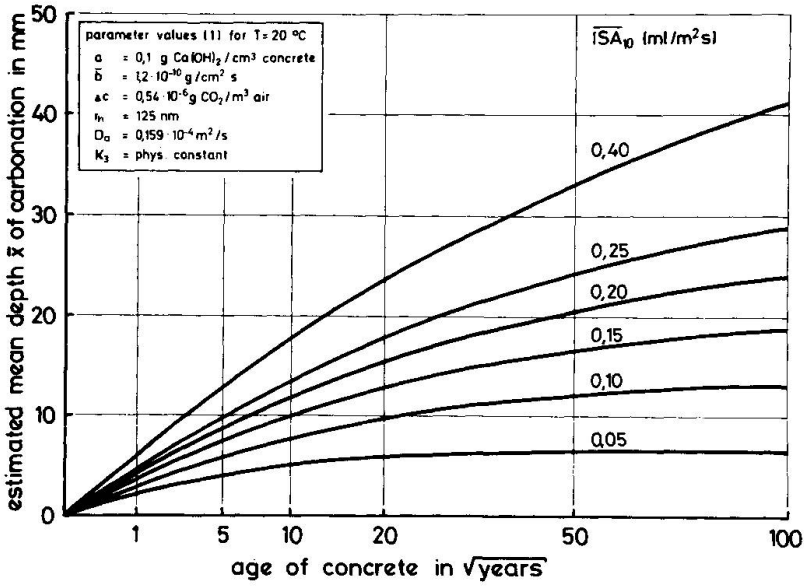

Fig. 1: Mean of carbonation depth dependent on age and ISA_{10}-value (Equ.(2) and (7))

The concrete cover also scatters [3]. Its 5 %-fractile may be expressed by

$$c_5 \approx 0{,}6\ \bar{c} \tag{9}$$

with $\bar{c}$, the nominal cover of bars to be ensured by spacers. Now, the durability criterion is expressed by:

$$x_{95}(t_1) \leq c_5 \tag{10}$$

with t_1, the service life.

This criterion is a rough simplification of reality because it stipulates a probability of 1 for the coincidence of peak values of carbonation depth occurring at the reinforcing bars placed with an unknown, distinct spacing.

3.2 Comparison with test results

Fig. 2 shows the dependence of test results of the mean carbonation depth on age for concrete walls exposed for about 25 years to weather. At the age of 25 years ISA-tests were performed on-site. With Equ.(7), (2) and with the mean experimental ISA-values the prediction curves x(t) and $x_{95}(t)$ can be calculated. For exposure to normal weather the minimum cover which corresponds to c_5 would have to be 25 mm acc. to DIN 1045. The example of Fig. 2 shows that peaks of carbonation would reach the steel's surface after ≈ 90 years.

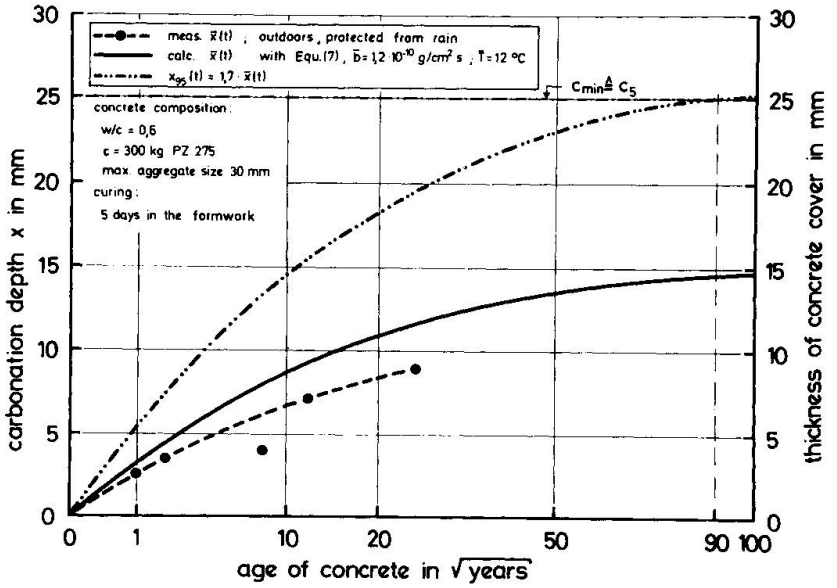

Fig. 2: Comparison of measured and calculated carbonation depth for a 25 years old concrete (calculation with measured ISA_{10}-value at 25 years)

3.3 Use of model in practice

The prediction model in combination with on-site ISA-tests can be used for: a) quality control in course of acceptance of the just completed structure and b) durability assessment of the older structure in course of maintenance. In any case reliable information on concrete cover is necessary.

For quality control certain mean ISA_{10}-values for acceptance must be stipulated which should not be transgressed by the on-site results.

In course of inspection of a structure, ISA-readings can be taken in suitable intervals. On their basis, carbonation can be estimated. By occasional measurement of the carbonation depth the model uncertainty can be reduced.

4. FINAL REMARK

The model presented is yet a tentative one. Several assumptions were necessary in course of its development. Thus, further evaluation is needed for its corroberation.

REFERENCES

[1] Schießl, P.: Zur Frage der zulässigen Rißbreite und der erforderlichen Betonüberdeckung im Stahlbetonbau unter besonderer Berücksichtigung der Karbonatisierung des Betons, DAfStb-Heft 255, 1976

[2] Rostásy, F.S.; Bunte, D.: Test methods for the on-site assessment of reinforced concrete surfaces exposed to normal weather, IABSE-Symposium Durability of Stuctures, Lisbon, 06.09. - 08.09.1989

[3] Stangenberg, F.; Kiefert, H.: Erfahrungen bei der Qualitätskontrolle von Stahlbetonbauwerken, Beton- und Stahlbetonbau 83, 1989, P. 53 - 58

Leere Seite
Blank page
Page vide

Influence of Local Repairs on Corrosion of Steel Reinforcement

Influence des réparations locales sur la corrosion des aciers d'armature

Beeinflussung der Korrosion der Bewehrung durch örtliche Instandsetzungsarbeiten

Joost GULIKERS
Civil Engineer
Univ. of Technology Delft
Delft, The Netherlands

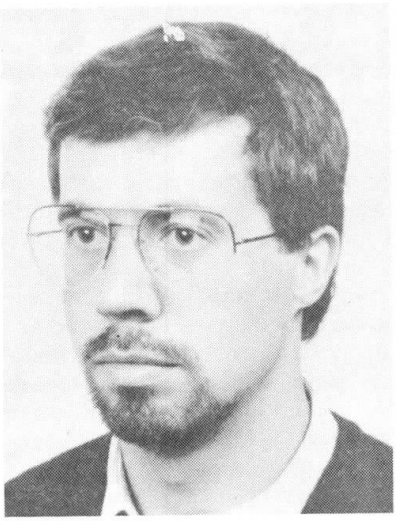

Joost Gulikers received his Master of Science degree at Delft University of Technology, The Netherlands, in 1986. Since then he is a research engineer at the Stevin Laboratory and is involved in research projects on durability of concrete structures.

SUMMARY

In this paper a description is given of a concrete corrosion celle which has been developed to investigate the mutual influence, between rebars in carbonated concrete and rebars embedded in repair mortar, on the corrosion processes. This influence is qualitively analyzed and preliminary test results are presented.

RÉSUMÉ

Une description est donnée d'une cellule d'essais de corrosion de béton permettant d'examiner l'influence mutuelle entre des barres enrobées de béton carbonaté et des barres enrobées de mortier de réparation, sur le processus de corrosion. Cette influence est analysée qualitativement et des résultats préliminaires sont présentés.

ZUSAMMENFASSUNG

Eine Betonkorrosionszelle wird zur Untersuchung der gegenseitigen Beeinflussung zwischen Bewehrung in karbonatisiertem Beton bzw. der Bewehrung umgeben von Reparaturmörtel und dem Korrosionsvorgang beschrieben. Diese Beeinflussung wird qualtitativ erfasst und vorläufige Versuchsergebnisse werden vorgelegt.

1. INTRODUCTION

Non-carbonated and chloride-free concrete normally provides reinforcement with excellent corrosion protection. The high alkalinity of the pore-water in concrete (pH > 12.5) results in the formation of a tightly adhering iron oxide film on the steel surface, preventing the ionic dissolution of iron. Corrosion of steel, however, can occur if the concrete is not of adequate quality, the structure was not properly designed for the service environment, or the environment was not as anticipated or changed during the service life of the concrete. Carbonation of concrete due to the ingress of carbondioxide from the air results in the reduction of the pH-value below 10, thereby permitting corrosion of reinforcing steel. The presence of chloride-ions in concrete can cause severe corrosion to occur when the chloride content at the steel surface exceeds a critical limit. The rate of corrosion is strongly influenced by environmental factors. Both carbonation- and chloride-induced corrosion can occur only if sufficient oxygen and moisture are available.
Because the corrosion products (rust) occupy a greater volume than the steel and exert substantial stresses on the surrounding concrete, corrosion results in deterioration of concrete. At the exterior surface this may demonstrate as staining, spalling and cracking of the concrete. Durability, structural and esthetic aspects can be the reason for repairing the damaged structure. If only a part of the total concrete surface is damaged it may be decided that only those parts should be repaired. In practice it is observed that local repairs can negatively affect the corrosion behaviour of rebars embedded in the non-repaired concrete. The effects of local repairs on the corrosion processes in carbonated concrete are studied by means of a concrete corrosion cell with which the influences of all relevant practical parameters can be quantitatively determined under different conditions. The principles of the corrosion cell will be described and the first results will be presented.

2. ELECTROCHEMICAL PRINCIPLES

Corrosion of steel in concrete is an electrochemical proces which can be divided in an anodic and a cathodic part: at the anode electrochemical oxidation takes place and at the cathode electrochemical reduction occurs. Any metal surface on which corrosion is taking place is a composite of anodes and cathodes being electrically connected through the body of the metal itself. At the anode, which is the negative pole, the dissolution of ferrous ions takes place as a result of the oxidation of iron:

$$Fe \rightarrow Fe^{+2} + 2e \qquad (1)$$

The ferrous ions are subsequently changed to oxides of iron by a number of complex reactions. At the cathode, which is the positive pole, reduction takes place. In a high alkaline environment and an adequate supply of oxygen, as is the case in concrete, the cathodic reaction is represented by:

$$2H_2O + O_2 + 4e \rightarrow 4OH^- \qquad (2)$$

If the cathodic process is the slower process, the corrosion is considered to be cathodically controlled. Conversely, if the anodic process is slower, the corrosion rate is said to be anodically controlled. In concrete, one or two types of corrosion-rate-controlling mechanisms normally dominate. One is cathodic diffusion, where the rate of oxygen diffusion through the concrete determines the rate of corrosion. The other type of controlling mechanism involves the development of a high resistance path. When steel corrodes in concrete, anodic and cathodic areas may be as much of several decimeters apart, therefore the resistance of the concrete may be of great importance [5].
The corrosion process can proceed only if certain conditions are fulfilled. For the situation where depassivation due to carbonation of the concrete has occurred, these principal conditions are shown schematically in fig. 1:
Anodes develop as a result of depassivation; cathodic reactions can occur in both passivated and depassivated areas of the steel surface when sufficient water and oxygen are available. The ferrous and hydroxyl ions dissolute in the pore water; the released electrons travel through the steel from the anode to the cathode nearby.
Depassivation of steel caused by carbonation of concrete leads to the formation of micro

corrosion cells on the steel surface. The cathodic and anodic reactions proceed directly side by side and will cause a uniform corrosion rate along the steel surface. Under certain conditions it may be possible that in carbonated concrete corrosion areas develop where the cathodic reactions dominate the anodic reactions. This overcharge of cathodic activity can support the anodic reactions in corrosion areas nearby.

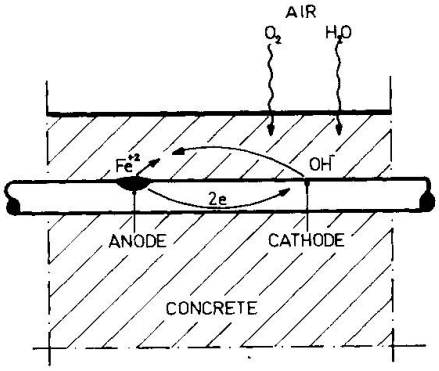

Anodic reaction
(oxidation)

$Fe \longrightarrow Fe^{++} + 2e$

Cathodic reaction
(reduction)

$2H_2O + O_2 + 4e \longrightarrow 4OH^-$

Fig. 1 Schematic representation of corrosion processes after depassivation by carbonation

The presence of chloride-ions in concrete usually gives rise to the formation of a macro-cell, i.e. localized anodic and cathodic regions of the steel surface are seperate from one another. This sitation is especially dangerous when large cathodic regions are opposed to small anodic regions. This so-called pitting corrosion results in a significant dissolution of metal advancing in the interior of the rebar.
In this paper repair of reinforced concrete with carbonation induced corrosion is subject of research.

3. EXPERIMENTS

3.1 Description of the concrete corrosion cell

The concrete corrosion cell is shown in fig. 2; a similar corrosion testing cell was previously developed by Schiessl [1]. Each specimen is made of solid concrete (see Appendix for composition and curing conditions) and contains initially 4 electrodes (steel rebars) at fixed places: 3 electrodes (A, B and D) at the upper surface with a concrete cover of 10mm and an

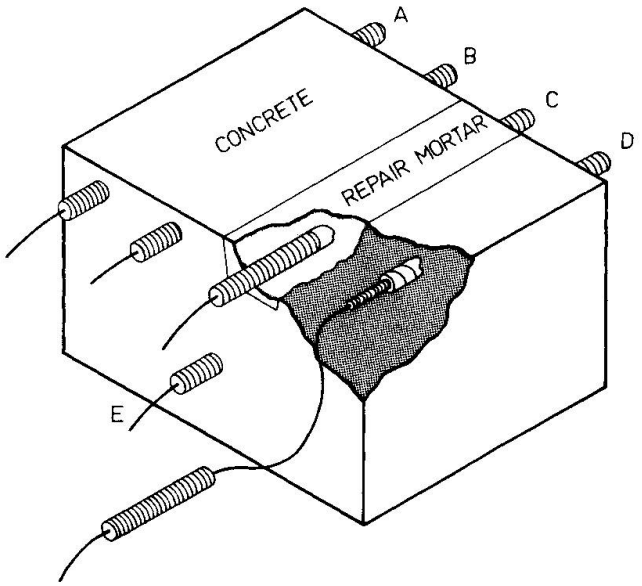

Fig. 2 Concrete corrosion cell

in-between distance of 50mm, and 1 electrode (E) at a distance of 50mm to the basis. At the upper surface a slot is made with a depth of 30mm. All electrodes have an effective corrosion length of 100mm and a surface area of $37.7*10^3 mm^2$. After accelerated carbonation (80 days at 5% (v/v) CO_2 and 50% R.H.) the three upper electrodes are positioned in carbonated concrete and as a consequence they are in a potential state of corrosion. Micro corrosion cells will develop dependent on the environmental conditions, viz. relative humidity and the availability of oxygen. The electrode E is surrounded by non-carbonated concrete and can act only as a cathode (macro cathode); this electrode is used for reference measurements. After accelerated carbonation the four vertical surfaces of the specimen are sealed with a tight epoxy coating permitting access of oxygen and moisture only through the upper and lower surfaces of the specimen. The electrodes are externally conductively connected, enabling the corrosion current to flow. Any corrosion due to micro cell formation cannot be detected until at the end of the test the specimens are split and the weight of rust for each electrode is determined.
In each specimen the electrically conductive connection between the electrodes A - B and D - E was established directly after the period of accelerated carbonation. After three months the fourth electrode (C) at the upper surface is placed in the slot and embedded in repair mortar. Two days after repair the connections between the electrodes A - B and C - D were established.
It is emphasized here that the only purpose of this type of concrete corrosion cell is to measure the mutual influence between rebars embedded in carbonated concrete and rebars embedded in repair mortar on the corrosion processes.

3.2 Description of the measuring system

To determine the very small corrosion currents a special developed measuring system is set up (see fig. 3). Each electrical circuit consists of two electrodes (A - B and C - D) which are continuously interconnected by means of a copper wire through a resistor. The resistance is relatively low to limit any external interference of the natural corrosion process; in the present situation a resistance of 1X is chosen. Between 10 corrosioncircuits and a multimeter (type: Philips PM 2535) 1 multiplexer (type: Philips PM 2121) is placed; in total 60 circuits are monitored. A PC (type: Hewlett Packard Vectra ES) is connected with the multimeter to start the measuring cyclus and to buffer the received corrosion current data.

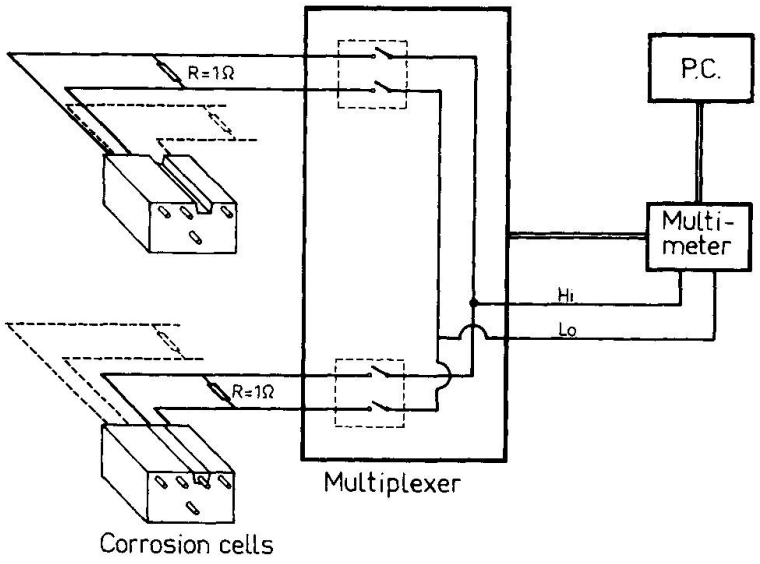

Fig. 3 Measuring system

3.3 Variables

In the first stage of the research program only two parameters are taken into account, viz. the relative humidity of the air and the type of repair mortar:

R.H. : 1) alternating climate : 2 weeks 50% R.H.;
2 weeks 100% R.H.
2) constant climate : continuously 80% R.H.

Repair mortar : 1) CC-mortar;
2) PCC-mortar;
3) PC-mortar.

4. PRELIMINARY EXPERIMENTAL RESULTS

The results of the first three weeks after repair are shown in figs. 4 and 5 for different climate conditions and different types of repair mortar.

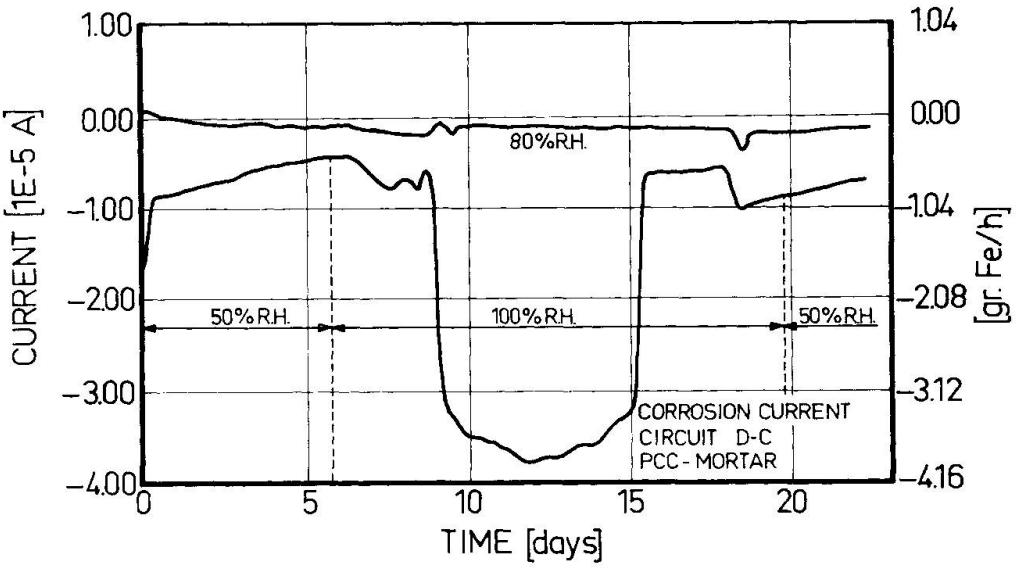

Fig. 4 Corrosion currents for PCC-mortar at 80% R.H. and 50/100% R.H.

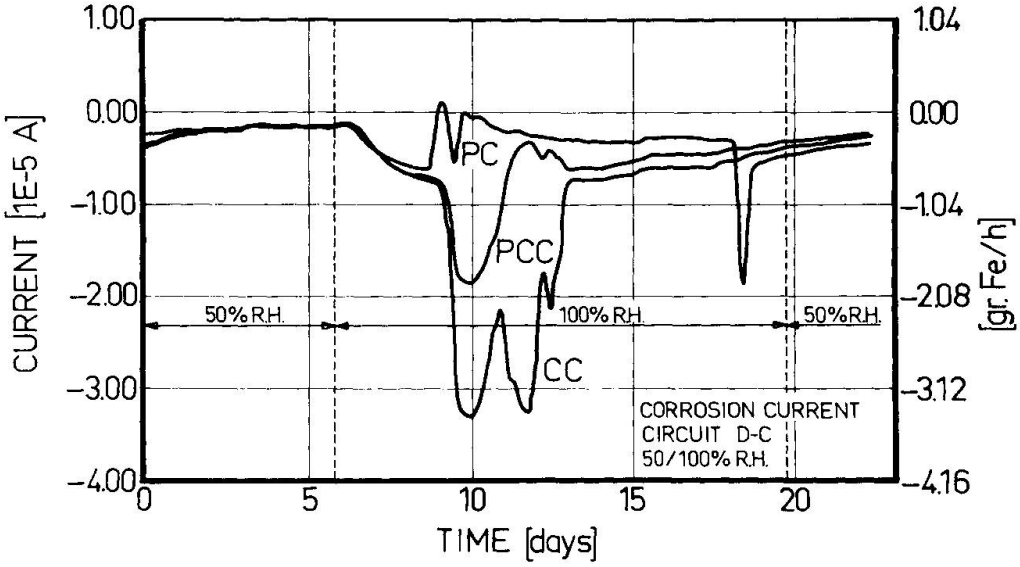

Fig. 5 Corrosion currents for 3 types of repair mortar at 50/100% R.H.

5. DISCUSSION

The steel reinforcement in the carbonated concrete area is in a potential state of corrosion; the steel surrounded by repair mortar cannot corrode i.e. at the steel surface no anodic reactions can proceed. In a mineral mortar (CC- and PCC-mortars) the alkaline environment re-establishes a protective oxide film on the steel surface (repassivation). In a PC-mortar, e.g. epoxy mortar, permeability and porosity are very low and as a result cathodic and anodic reactivity will be very slow. Rebars embedded in mineral mortars can develop into macro cathodes, the rate of their reactivity being mainly determined by the diffusion of oxygen. When these macro cathodes are electrically connected with rebars in carbonated concrete an acceleration of their anodic processes will occur. This can be especially dangerous if the acceleration is concentrated on a small steel area. In that case a situation identical to pitting corrosion is possible. For rebars partly embedded in repair mortar and partly in carbonated concrete it is likely that the small macro anode will occur next to the large macro cathode. Whether cathodic or anodic reactions dominate at steel surfaces of rebars surrounded by PC-mortar mainly depends on the porosity and permeability of the repair mortar and the corrosion controlling factors at the rebars in carbonated concrete nearby.

In the period about which tentative results are presented, the measuring system is tested and further developed; the time period is too short to draw any definite conclusions from the results. The program is continued to investigate the long-term effect of local repairs on corrosion processes; in due time these results will be presented and discussed.

ACKNOWLEDGEMENTS

The experiments in this research project are carried out in the Stevin Laboratory of the Delft University of Technology. Support provided by the CUR (Centre for Civil Engineering Research, Codes and Specifications) is acknowledged with thanks.

REFERENCES

1. SCHIESSL, P.; SCHWARZKOPF M., Chloride-induced corrosion of steel in concrete: Development of a concrete corrosion testing cell. Betonwerk + Fertigteil-Technik, Heft 10/1986.

2. SCHWENK W., Principles of the corrosion-chemical behaviour of structural steel. Betonwerk + Fertigteil-Technik, Heft 4/1985.

3. GONZALEZ J.A.; ALGABA S.; ANDRADE C., Corrosion of reinforcing bars in carbonated concrete. British Corrosion Journal, No.3 1980.

4. HOPE B.; IP A., Corrosion of steel in concrete made with slag cement. ACI Materials Journal, November/December 1987.

5. ACI Committee 222, Corrosion of metals in concrete. ACI Journal, January/February 1985.

6. RILEM Technical Committee 60-CSC, Corrosion of steel in concrete. State of the art report, Final draft, April 1986.

APPENDIX

Concrete composition: 300 kg/m^3 bfsc; wcf = 0.60; aggregate 8-16mm: 24%; 4-8mm: 20%; 2-4mm: 20%; 1-2mm: 10%; 0.5-1mm: 9%; 0.25-0.5mm: 9%; 0.125-0.25mm: 8%.
Curing conditions: 2 weeks 100% R.H.

Surface Shrinkage of Concrete: Evaluation and Modelling

Retrait superficiel du béton: évaluation et modélisation

Oberflächenschwinden des Betons: Ermittlung und Modellierung

Charles ABDUNUR
Docteur es Sciences
LCPC
Paris, France

Paul ACKER
Docteur de l'ENPC
LCPC
Paris, France

Bu-quan MIAO
Docteur de l'ENPC
LCPC
Paris, France

SUMMARY

The mechanical effects of drying shrinkage were investigated in the field and the laboratory, using theoretical, experimental and technological means. Direct stress measurements, by the stress release method, and their numerical analysis gave the stress profiles and the depth of damage for different configurations. Simulation of the drying effects by a stochastic model reproduced the same stress profiles. The explanation and evaluation of these effects should lead to appropriate precautions, for reinforcement protection and a better durability.

RÉSUMÉ

Les effets mécaniques dûs au retrait de dessiccation ont été étudiés, sur ouvrages réels et en laboratoire, associant des moyens théoriques, expérimentaux et technologiques. Des mesures directes de contraintes, par la méthode de libération, et leur analyse numérique ont permis de déterminer les profils de contraintes et la profondeur d'endommagement, pour différents configurations. Une simulation des effets du séchage par un modèle stochastique a reproduit les mêmes profils de contraintes. L'explication et l'évaluation de ces effets devraient faciliter la définition des précautions à prendre, pour la protection des armatures et une meilleure durabilité.

ZUSAMMENFASSUNG

Die Wirkung des Schwindens infolge Austrocknung wurde an Hand von Labor- und Bauwerksuntersuchungen erforscht. Dazu wurden drei verschiedene Studien durchgeführt; experimentelle, theoretische und technologische Studien. Direkte Spannungsmessungen mit flachen Druckmessdosen und ihre numerische Analyse haben die Bestimmung des Schwindens ermöglicht. Eine Simulation des Trocknungsvorganges durch ein stochastisches Modell hat die Ereignisse bestätigt. Durch die nun mögliche Erklärung und daraus resultierende Berechenbarkeit dieser Wirkung kann eine bessere Dauerhaftigkeit gewährleistet werden.

1. INTRODUCTION : EXTENSIVENESS OF CONCRETE SKIN CRACKING

In most concrete formulae, the water quantity necessary for the mix greatly exceeds that needed for the cement hydration. As soon as shuttering is removed, even in humid climates, a part of the water will migrate to the outside. This drying can attain a 5% loss of the total concrete weight and lead to considerable dimensional variations. Drying is never uniform and its effects have three components :

- eigenstresses, due to very slow drying and resulting gradients ;
- skin cracking of evolutive depth ;
- apparent strains, usually known as drying shrinkage.

These depend on the geometry of the sample or structural element. By their intense superficial mechanical effects, both the removal of shuttering and the variation of air humidity are equivalent to a thermal shock. In general, the result is a pattern of very dense, shallow hair cracks which do not always jeopardize the durability of the material. However, under certain conditions, an extensive growth of this cracking can favour reinforcement corrosion, a very frequent type of pathology cases in concrete structures.

To better control this mechanism, it could be helpful to first evaluate the mechanical effects of shrinkage with the utmost possible accuracy.

2. A DOUBLE APPROACH BY EXPERIMENT AND MODELLING

Many authors [1], [2], have given a fair but rather qualitative description of these effects. By thermal analogy, shrinkage strains and eigenstresses cannot be properly calculated from measured water content distributions (fig. 1), owing to the lack of a sufficiently accurate "coefficient of hydric contraction". This can only be obtained on a test sample free from gradients and cracks, which are difficult to avoid, given the excessively slow drying process [3].

For a quantitative analysis of the mechanical effects, we needed an accurate method of direct stress measurement, leading to a more realistic constitutive model. It happens that such a method has already been developed by one of the authors [4], [5], for the assessment of structures. It now offers a suitable means for this quantitative approach.

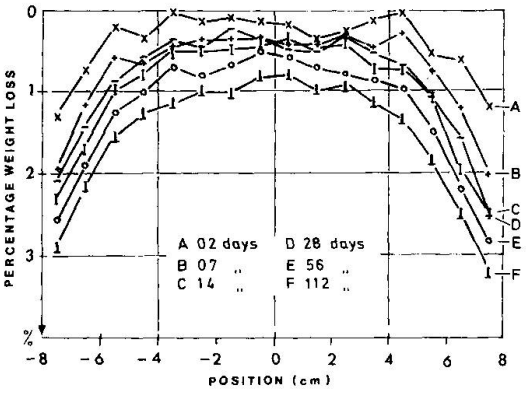

Fig. 1 : Time-dependent distribution curves of water content measured in a 10-cm-diameter, 16-cm long concrete core, laterally coated to represent uniaxial drying in a 16-cm thick infinite slab.

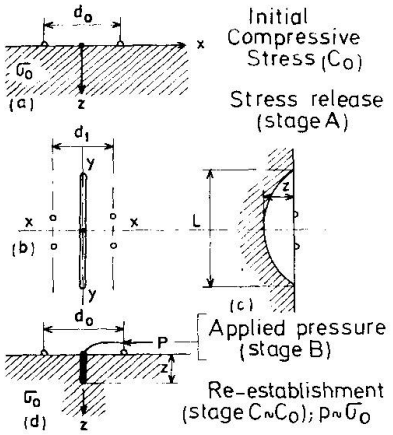

Fig. 2 : Different stages of direct stress measurements, by the release method.

3. DIRECT MEASUREMENT OF STRESS

3.1 - The release method

It is a local and partial release of stress, followed by a controlled pressure compensation [5]. In practice (fig. 2 and 3), a displacement reference field is first set up on the surface ; a tiny slot is then cut in a plane normal to the desired stress direction ; finally, a special very thin flat jack is introduced into the slot and used to restore the initial displacement field. The amount of cancelling pressure gives the absolute compressive stress normal to the slot. In the same way, with the same accuracy, tensile stresses are obtained by a corollary. The stress profile is traced by repeating the operation at closely successive depths of the same slot, then by treating the data numerically. In spite of the minute working scale, the error stays within 0.3 MPa. The depth operating range is 80^{mm}, giving an average stress till 32^{mm}. Measurement is "direct" in the sense that the same physical quantity is involved (pressure for stress) and that none of the material elastic properties are needed. These are even determined in the process. Stress components may sometimes be separated.

3.2 - Applications on site

The first operational field application of the release methode was on a 10-year-old tall concrete column with a box section [6]. It carries two half, simply supported spans of a bridge (equivalent to 2.5 MPa) and undergoes a slow, irregular foundation settlement. On four points of the section, absolute stress profiles were determined through the outside part of wall thicknesses (fig. 4). At all four points, contrary to what is expected from a compression member, high tensile stresses were measured close to the surface, falling sharply with depth.

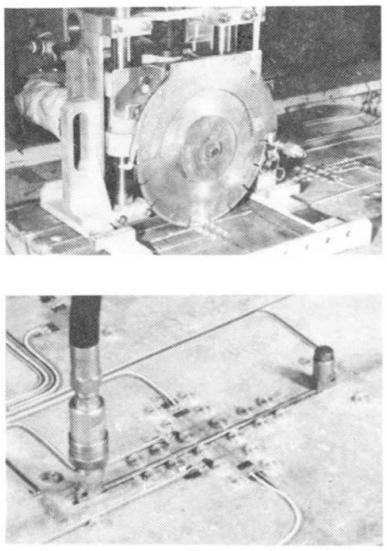

Fig. 3 : (top) Slot cutting machine with 0.1-mm adjustment ;
(bottom) A 0.1 µm-precision displacement measuring apparatus with a 4-mm thick flat jack in the slot.

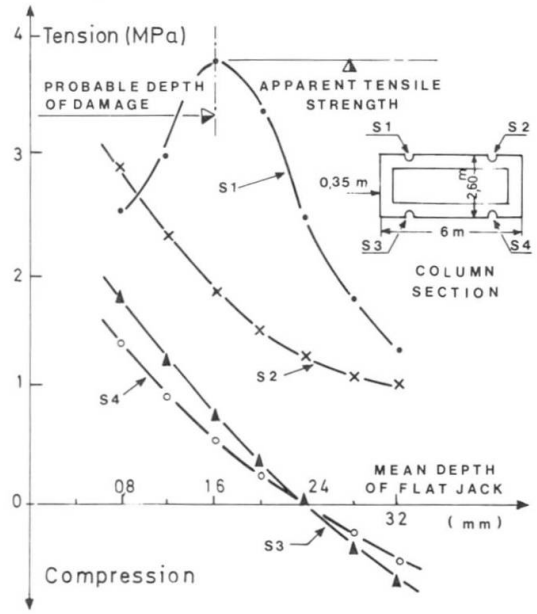

Fig. 4 : Compensating pressures, given by the release method, reflecting the actual stress profiles on a 10-year-old concrete column with a 2.5 MPa external compression. They show the still prevailing superficial tensions and sharp gradients of shrinkage. The relative vertical shift between the curves, illustrates the effect of flexure (confirmed later while completely cutting and shoring the column base).

Shrinkage effect is undoubtedly the cause, running deep with similar gradients and stabilizing beyond the range of measurement. At point S1, the stress curve breaks right below the usual tensile strength of concrete, announcing a softening of stress by superficial cracking. The measured stress at this depth is in fact an average over the area of the flat jack, hence the actual stress distribution should be more pronounced upwards.

Such applications helped to emit basic and realistic assumptions necessary to carry on the research.

4. LABORATORY TESTS AND A MODEL FOR ANALYSIS

Three plain concrete test slabs were casted, 80 x 40 cm, respectively 8, 10, 16 cm thick [7]. The first one had a uniform 12.5 MPa prestress at 7 days. In areas away from edges, stress distribution is assumed to depend exclusively on the distance from the surface.

The release method was used again in all slabs. The displacement field evolution, accurately measured as cutting proceeded, was combined with a specific compliance matrix (F.E.M. 3-D programme CESAR), to obtain a better defined stress profile as a function of depth. In this analysis model, elastic behaviour is assumed, as confirmed by the linear and reversible response of the displacement field to the flat jack pressure, at consecutive slot depths.

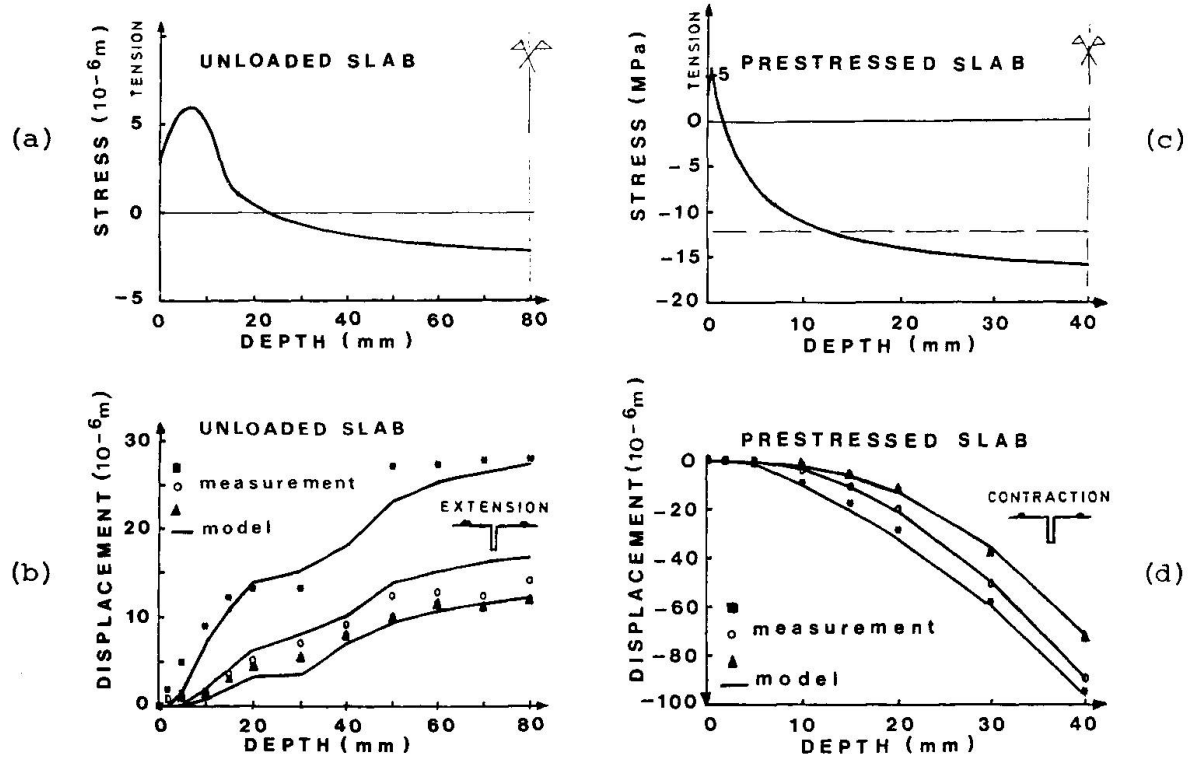

Fig. 5 : (a, c) Stress distribution, in non-loaded and prestressed configurations, estimated by the analysis model, completed by parametric optimization.
(b, d) Respective surface displacements comparing those actually measured by the release method (points), and those deduced from stress distributions (curves). In the two-step evolution observed in (b), the first discontinuity marks a stress fall to zero, the second, an opposite flexure effect of stress redistribution after partial release in a slab of limited cross-section.

5. RESULTS AND DISCUSSION : HIGH STRESSES, SOFTENING AND LOAD COUPLING

The resulting stress profiles and the comparison of measured and computed surface displacements are given in fig. 5. Considerable surface displacements were observed, depending heavily on the external loading configuration.

In the non-loaded slab (fig. 5b), the increasing depth-dependent extension reflects an intense superficial tension of several MPa's. A direct resolution by the above analysis model gave the general form of this tension which rises first with depth, passes by a maximum, then falls to compression, in the central part of the thickness, to sum up the internal forces over the cross-section to zero. The presence of a softening zone confirms earlier stress measurements on structural members with low compression loading (curve S1, fig. 4). The shrinkage stress profile may now be assimilated to a junction of two curves : (i) a parabola, covering the damaged depth, with its vertex on the tensile strength level and (ii) a central curve, proportional to the water content distribution.

Very close to the surface, the analysis model grows too delicate to apply owing to the extremely small compliance coefficients. The damaged depth then becomes the main parameter whose optimum value should fix the stress curve and give the best correlation between the theoretically deduced displacements and those actually measured by the release method (fig. 5b, d). The optimization process yielded a 4.0 and 6.4 mm damage, respectively for the 10 and 16 cm thick non-loaded slabs. It is 0.3 mm only for the prestressed slab. With these additional and consistent data, the stress profiles (fig. 5a, c) were obtained.

The main difficulty of the above approach naturally resides in the lack of a reliable constitutive law for concrete in tension. On this scale, the experimentally observed softening strongly depends on the size of discontinuities [8]. This size effect may be explicitly reproduced in Rossi's stochastic model [9]. Specific, perfect brittle, contact elements are inserted in an elastic F.E.M. model with tensile strength values placed at random according to an experimentally determined statistic distribution. In applying this model to the above example fig. 5 b, the stochastic mean stresses generate a shape similar to the experimental distribution (fig. 6).

At successive drying stages, the model shows a "condensation" process of main crack openings : as damage deepens, fewer cracks propagate giving more concentrated, hence wider, openings.

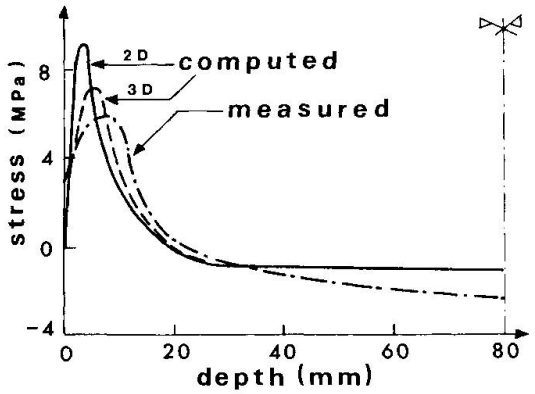

Fig. 6 : Depth-dependent mean stresses, computed by the stochastic model and compared to experimental values for the 16 cm thick test slab.

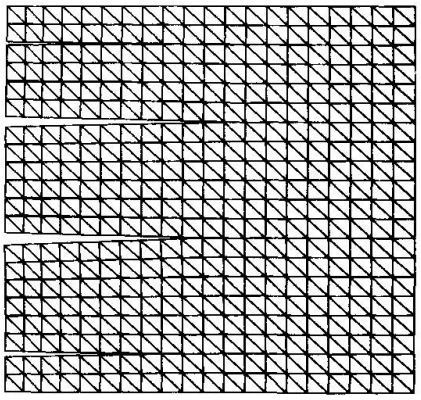

Fig. 7 : Crack pattern obtained by the stochastic model. Cracking depth varies from 5 to 11 mm but only a few cracks appear open.

Finally, in the prestressed slab, even a 12.5 MPa applied compression could not prevent a slight tension damage experimentally observed. However, this loading did favour an almost full development of the intrinsic drying strains. These reflect the water content distribution and proportionally induce the stress profile (fig. 5c) deduced through the release method.

6. CONCLUSIONS

1- The displacements, occuring on the concrete surface while cutting a slot, reflect the high tensile stresses due to drying shrinkage and enable their evaluation.
2- The observed displacement field response to stress release is significantly different according to whether concrete is prestressed or not. In both cases, the response to jack pressure confirmed the linear elastic relationship assumed between drying strains and stresses.
3- A closer scrutiny of the results shows potential tension exceeding the strength of the material through an appreciable depth (5-10 mm), and creating a damage or softening zone.
4- The quantitative analysis of the mechanical damage, actually suffered by the concrete skin layer, confirms the importance and facilitates the optimization of two re-bar parameters : cover and bond. This may contribute to a better control of durability problems linked with the drying of concrete.
5- The stress release method, developed in the LCPC, proved suitable for the analysis of drying effects. The method also enables the access to external load stresses acting on the structure, for a drying depth within the measurement range. For drying beyond this range, other operation ways are now being tested to attain the load stresses.

ACKNOWLEDGEMENTS

Part of this research was supported by AFREM-MRT-DAEI Contract.
The authors thank A. Lelièvre and A. Attolou for the care with which they carried out the tests.

REFERENCES

1. WITTMANN F.H., ROELFSTRA P.E., "Total Deformation of Loaded Drying Concrete", Cement and Concrete Research, Vol. 10, p. 601-610, 1980.
2. BAŽANT Z.P., RAFTSHOL W.J., "Effect of Cracking and Drying in Shrinkage Specimens", Cement and Concrete Research, Vol. 12, n° 2, 1982.
3. MENSI R., ACKER P., ATTOLOU A., "Séchage du béton : analyse et modélisation", Matériaux et Constructions, Vol. 21, p. 3-12, 1988.
4. ABDUNUR C., "Stress and Deformability in Concrete and Masonry", IABSE Symposium, Final Report, p. 123-130, Venezia, 1983.
5. ABDUNUR C., "Mesure de contraintes sur ouvrages d'art par une méthode de libération miniaturisée", Bulletin de Liaison des LPC, n° 138, p. 5-14, 1985.
6. ABDUNUR C., "Mesures directes de contraintes sur une pile du viaduc de Charmaix", Rapport LCPC, 1986.
7. MIAO B., "Effets mécaniques dus au retrait de dessiccation du béton", Thèse de l'ENPC, Paris, 1988.
8. Proc. CNRS-NSF Workshop "Localization, Damage and Size Effect", J. Mazars and Z.P. Bažant Ed., Elsevier Publ., 1989.
9. ROSSI P., PIAU J.M., "The Usefulness of Statistical Models to Describe Damage and Fracture in Concrete", in Workshop ref.8.
10. ACKER P., "Comportement mécanique du béton : apports de l'approche physico-chimique", Rapport de Recherche des LPC, n° 152, 1988.

Thermal Incompatibility of Concrete Components and Durability of Structures

Incompatibilité thermique des composants du béton et durabilité des structures

Thermische Unverträglichkeit der Betonkomponenten und Dauerfestigkeit der Konstruktionen

Srdjan D. VENEČANIN
Docent
University of Beograd
Beograd, Yugoslavia

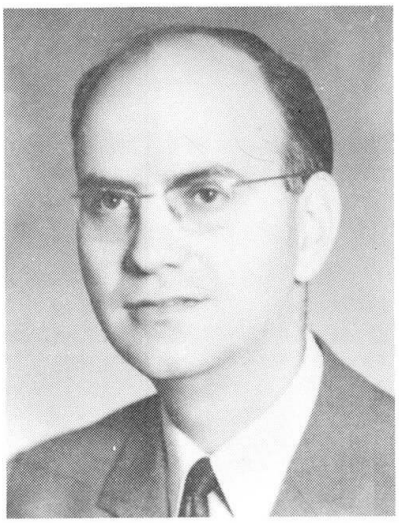

Srdjan Venečanin, born 1930, received his civil engineering degree at the University of Beograd, Beograd, Yugoslavia. He has designed reinforced and prestressed concrete structures. Now he lectures on Concrete Bridges at the Dep. of Civil Eng. of the University of Beograd. His research work is associated with durability of concrete structures.

SUMMARY

Unequal thermal expansions of aggregate and hardened cement paste reduce durability of concrete if it is exposed to temperature changes. Properties of aggregate which affect this phenomenon, and types of structures in which this phenomenon can appear are discussed.

RÉSUMÉ

Les dilatations thermiques différentes des granulats et de la pâte de ciment durcie réduisent la durabilité du béton s'il est exposé à des variations de température. Les propriétés des agrégats influençant ce phénomène ainsi que les types de structures concernés, sont décrits dans l'article.

ZUSAMMENFASSUNG

Die ungleichen Volumenänderungen der Zuschlagstoffe und der Zementkörner infolge von Temperaturänderungen verkleinern die Dauerfestigkeit des Betons. In der vorliegenden Arbeit wird über die Eigenschaften der Zuschlagstoffe, welche diese Phänomene beeinflussen, sowie über die Art der Konstruktionen, bei welchen sich derartige Fragen stellen, diskutiert.

1. INTRODUCTION

Unequal temperature volume changes of concrete components - aggregates and hardened cement paste - cause tensile stresses and cracks in concrete. This does not reduce much compressive strength, but cracks enable penetration of moisture and chlorides into concrete, and durability of such concrete is reduced.

This phenomenon is often called thermal incompatibility of concrete components (TICC). It appears if difference of coefficients of thermal expansion (CTE) of concrete components is sufficiently large, and if such concrete is exposed to sufficiently large temperature changes.

2. SHORT BACKGROUND

One of the first papers on TICC /1/ describes rapid failure of some cast stone steps in the winter 1938-39. An aggregate of unusually low CTE was used. The published discussion /2/ by ten writers was approximately five times as large as the original paper, and it shows the great interest for the theme.

In the last five decades the problem was discussed in journals, but "investigations in the literature and authoritative textbooks on the subject do not present a clear-cut picture of the effects that might be expected and some aspects of the problem are somewhat controversial" /3/. In fact some experiments confirmed theories on TICC, but some did not.

In the last ten years or so, analytical solutions supported the theories on TICC phenomenon /4, 5, 6/, and recent laboratory tests /7, 8/ and tests with concrete drilled from bridges /9/ absolutely confirm detrimental effects of TICC. Doubts that in specimens of young concrete, when exposed to temperature changes, are exposed to the effects of autogeneous healing and faster hydration during "hot" part of temperature cycles, which also were discussed in the literature /10/, have been taken into account: in specimens of young concrete, when exposed to large number of temperature cycles, and in old concrete drilled from bridges, there is no interference of autogeneous healing or faster hydration of cement.

A rewiew of the problem of TICC is given in the literature /11/.

3. MAIN THERMAL PROPERTIES OF COMPONENTS THAT AFFECT TICC

CTE of hardened cement paste varies between 9 and 25.4×10^{-6}/K, which is not large interval /12/. CTE of rocks which are usually used as aggregate in concrete, varies between negative values - contracting when heated - and 16×10^{-6}/K - see /12/.

However, carbonate rocks, which have very low values of CTE, sometime have nonelinear relationship between strains and temperature; they are often nonhomogeneous to a high degree; after cyclic temperature changes they may have residual strains; and often they are more or less thermally anisotropic. All of these properties are important for the phenomenon of TICC, and it is obvious that they have to be studied, and that they make CTE very poor tool to describe thermal volume changes of carbonate (and some other) rocks.

Nonelinear relationship means that inside a temperature range of, say, 100 K, CTE can be lower and higher, for some subintervals, than the average value for the whole range. Usually for the lower temperatures CTE of limestones is lower - which means that damaging effects of TICC could be bigger at lower temperatures.

Nonhomogeneity means that average value of CTE should be measured with as much as possible readings. Special technique has been devised: cube rock specimens have been used to measure temperature strains on each cube face in four directions - 24 readings at each temperature level per specimen (see e.g. /9/).

Residual strains after cyclic temperature changes mean different coefficients of thermal contraction. Since after each temperature cycle new residual strains can appear, this means different CTEs after each cycle - up to a point when these

residual strains between two subsequent cycles reduce to zero!

Thermal anisotropy mostly depends on orientation of calcite minerals - since calcite crystals are thermally anisotropic: they expand in the direction of one crystallografic axis, and contract in the directions of other crystallografic axes. If calcite crystals in the rock are oriented in the same direction, they transfer this anisotropy to the rock. This parallel orientation is often present to some degree, and degree of thermal anisotropy of the rock depends on the degree of parallel orientation of calcite crystals in it. The higher the thermal anisotropy of aggregate rock, the higher are the damaging effects of phenomenon of TICC. It is quite possible that the average value of CTE of a rock is rather near to that of hardened cement paste, but that damaging effects of TICC are high because thermal anisotropy of aggregate rock is high.

4. MECHANISM OF DETERIORATION OF CONCRETE DUE TO THE TICC

Generally TICC do not have to reduce much compressive strength of concrete. However it causes cracks in the concrete, mostly bond between aggregate and hardened cement paste is broken, and then moisture or chlorides penetrate concrete and damage it. So it is quite possible that TICC alone is not able to damage concrete significantly, and that frost action or chloride action is not able to damage concrete alone, but when TICC is combined with one of these two actions, concrete can be damaged. Combination of two or more adverse actions exponentially raises possibilities of damages of concrete.

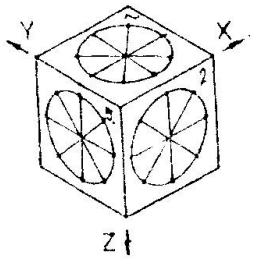

Cube rock specimens measuring temperature strains parallel to the cube edges and in the directions of diagonals

5. TYPES OF CONCRETE STRUCTURES IN WHICH TICC CAN BE DANGEROUS

It is necessary that components of concrete change their volumes differently when exposed to temperature changes. So the structure must be exposed to temperature changes beside having components of different thermal properties. Such types of structures are bridge decks, concrete roadways, concrete airport runways, taxiways and aprons, industrial chimneys, prestressed concrete pressure vessels, cryogenic concretes, roof tiles, and other concretes exposed to temperature changes.

If climatic conditions are severe, like in the Middle East desert regions where daily temperature changes can be large, or in Alaska or Siberia where seasonal temperature changes are large, all concretes exposed to the sun rays could be damaged by TICC. In some cases direct sun rays cause concrete surface to have nearly 30 K higher temperature than the air temperature is.

5.1 Bridge decks

Great surface of bridge slabs is exposed to direct sun rays, and temperature measurments show great differences of slab temperature and temperature of other parts of concrete bridge. This means that concrete of a bridge slab is exposed to rather large temperature changes - larger than the changes of the surounding air's temperature.

Cores drilled from the slab of a ten years old bridge were exposed to the temperature changes between -20°C and +60°C for 28 days - two complete thermal cycles per day. Then four of these cores, and four of reference ones, drilled from the slab of the same bridge - but kept at room temperature, were exposed to water pressure for a week: each day water pressure has been raised for one atmospehere, and kept seven hours per day under pressure. In the first four cores penetrated 72% more water than in the reference ones. It was obvious that new cracks deve-

loped in the specimens which have been heated and cooled in the thermal chamber.

CTE of limestone that has been used as coarse aggregate for this bridge has been measured for the temperature range between -20°C and +65°C, and was found to be about $3x10^{-6}$/K. Such a low CTE of coarse aggregate, and developement of new cracks in the bridge cores, show that TICC considerably contributed to the degradation of the bridge concrete /9/.

5.2 Concrete pavements

Concrete exposed to the direct sun rays reaches considerably higher temperatures than the surounding air. This means that range in which temperature of this concrete changes during one day is higher than diurnal temperature changes of the air. For concrete pavements this is very important because these concretes are exposed to the sun with great area, and TICC effects are to be expected /13/.

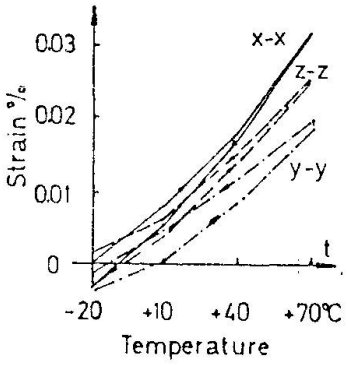

Strains vs temperature for three orthogonal directions shows thermal anisotropy

Contractors prefer to use limestones for concrete pavements because this kind of aggregate usually gives excellent compressive strength, even excellent tensile strength of concrete - and owner of the works require mostly control of compressive strength after 28 days. However limestones are the rock type which can have extremely low CTE - and combination of low CTE of aggregate and large range of temperature changes are essential conditions for detrimental effects of TICC.

Large milage of concrete pavement in Missouri, where it was noted that desintegration characterized initially by a typical map-cracking, occurred only when a specific kind of coarse aggregate has been used in concrete - has been reported by Reagel and Willis in their discussion /2/ of the paper /1/. Detrimental effects of TICC have been suspected, but Reagel and Willis note that it was found that most serious desintegration was always associated with the use of an aggregate having a large CTE. But they also note that this could be explained by more factors and phenomena whose effects overshadow any effect of thermal expansion.

Difficulties in separating effects of TICC and, for example, autogeneous healing, higher rates of hydration during "hot" part of temperature cycle (in experiments with young concrete), or "rim reaction", resulted in contradictory results of tests, and authoritative textbooks on the subject show some reserve when discussing this problem.

In the case of the Missouri pavements, thermal anisotropy of aggregate could also be the reason of desintegration of concrete.

5.2 Prestressed concrete pressure vessels (PCPV)

Since the first nuclear reactor with PCPV came into operation in France in 1959, the normal operating pressures and temperatures for this kind of structure have been gradually rising. Today operating pressures are of the order of 10 MPa, and operating temperatures of concrete reach 100°C - the steel liners reaching 300°C or even more.

Thermal gradient in PCPV requires high amount of prestressing steel around the vessel, but the lower CTE of the concrete, the lower amount of prestressing steel is needed. So often limestone of low CTE is used as crushed aggregate for concrete of PCPV - and problem of TICC is neglected. The same reasons apply for nuclear containment vessels.

To save on prestressing steel in such a way is a dangerous thing because low CTE of concrete is obtained by using aggregate of low CTE, making difference of CTEs

of aggregate and hardened cement paste bigger - and enhancing detrimental effects of TICC. When TICC starts cracking in such concrete, then "gas in cracks" loading problem, arising from leaks in the steel liner, exponentially raises possibilities of leakage of radioactive gasses outside the vessels.

The point is that TICC problem can be solved only by using concrete components of approximately the same CTE, and problem of stresses due to the thermal gradient can be solved by adding more prestressing steel - and not only by using concrete of low CTE. Conclusion should be that using thermally compatible concrete components means more prestressing steel, but it means less trouble during operation of reactor: less shutdowns during operation due to the leakage of radioactive gasses, and less consequent damages to the environment, etc.

5.4 Industrial chimneys

Though modern industrial chimneys have more than one flue in the exterior reinforced concrete shell, and the flue gasses are too hot and need liners, concrete shell still has higher temperature than the surrounding air. The temperature of exterior concrete shell is often changing, especially in higher parts of the chimneys, where constantly changing winds change concrete temperature. If concrete of such a chimney shell is made of thermally incompatible components, the cracks will appear soon.

The problem is rather similar as in PCPV: temperature gradient requires more reinforcement if CTE of concrete is higher - and vice versa. So it happens that some designers and contractors prefer limestone of low CTE for concrete aggregate, because this relults in concrete of low CTE, and save on reinforcing steel. However, this means trouble during operation of the plant - and, possibly, shutdowns and repairs of concrete.

5.5 Roof tiles

Measurements of temperature of roof covers which are exposed to sun rays show sometimes 40 - 50 K higher temperatures than the air. Cloudy weather affect temperature changes: some measurements have shown changes of 17 K in 7.5 minutes. The rain could be the reason of fast temperature changes of surfaces exposed to sun rays: some measurements have shown 8.3 K changes in only one minute, and 37 K in 30 minutes, of the surface hot due to the sun rays, when it was exposed to the rain.

Such severe conditions must destroy composite material if it consists of components with different CTE. If roof tiles are made of sand and cement, the sand should be quartzitic - with high CTE, which is near to the CTE of hardened cement paste.

Replacement of asbestos fibres by polymer fibres should cause trouble, because polymers usually have very high CTE, much higher than the CTE of hardened cement paste.

5.6 Concrete structures at cryogenic temperatures

Concretes exposed to cryogenic temperatures exhibit irregular volume changes when cooled: usually roughly between $-20^{o}C$ and $-70^{o}C$ concrete expands when cooled! Namely hardened cement paste expands when cooled, while nothing similar happens to the aggregate. This means great influence of TICC - and independently of the type of agregate, large tensile stresses and corresponding cracks appear. This is probably one of the main reasons why compressive strength of concrete decreases very much after only few temperature cycles in this range. Type of cement, moisture content, and pore structure are the factors affecting this phenomenon.

6. SOME CONSLUDING REMARKS

The problem is that nobody measures CTE of aggregate which will be used for a concrete. So there is no possibility at all to suspect TICC effects when concrete cracks. And everybody can see moisture or salts, and ascribe cracking to frost or chloride actions, or to something else.

Concrete structures described in Section 5 of this paper could be affected by TICC, but all kinds of concrete structures exposed to temperature changes could be affected by TICC - e. g. industrial floors.

If limestone aggregate is to be used for a structure which will be exposed to temperature changes, CTE of this rock should be measured for the temperature range in question. Also other properties discussed in Section 3 of this paper should be checked.

Practically all climatic conditions similar to the ones prevailing in the desert regions of the Middle East require cautiosness with respect to TICC.

Rocks containing silica minerals should be good with respect to TICC because they have high CTE - near to the CTE of hardened cement paste.

REFERENCES

1. Pearson J. C., A Concrete Failure Attributed to Aggregate of Low Thermal Coefficient. ACI Journal, Sept, 1941.
2. Hornibrook F. B. et al, Discussion of paper /1/, ACI Journal, June 1942.
3. Discussion of papers Nos. 8284 & 8302 by P. G. Fookes & I. E. Higginbottom, Proc. ICE; Part 1, August 1981.
4. Venečanin S. D., Influence of Temperature on Deterioration of Concrete in the Middle East, Concrete (London), August 1977.
5. Venečanin S. D., Durability of Composite Materials as Influenced by Different Coefficients of Thermal Expansion.ASTM STP 691, 1980.
6. Venečanin S., Analysis of Thermal Stresses in Concrete When it is Treated as Nonhomogeneous Three-component Composite Material (in Serbo-Croatian with summary in English). Proc. Symp. Yugosl. Soc. Structural Engineers, Trogir 1980.
7. Al-Tayyib A. J. et al, The Effect of Thermal Cycling on the Durability of Concrete Made from Local Materials in the Arabian Gulf Countries. To be published in Cement and Concrete Research.
8. Baluch M. H. et al, Concrete Degradation due to Thermal Incompatibility of its Components. IABSE Symp. on Durab. of Structures, Lisbon 1989.
9. Venečanin S. D. & Kovačević T. M., Thermal Incompatibility of Concrete Components in Concrete Bridges. Proc. Vol. III, First RILEM Congres, Versailles 1987.
10. Venečanin S. D., Experimental Study of Thermal Incompatibility of Concrete Components. III Int. Conf. on the Durab. of Build. Mat. & Comp., Proc. Vol. III, Helsinki 1984.
11. Venečanin S. D., Influence of Thermal Incompatibility of Concrete Components on Durability. The Arab. Journ. for Science & Engineering, Vol. 11, No., 2, 1986.
12. Venečanin S. D., Stresses in Concrete due to the Thermal Incompatibility of its Components. Int. Conf. on Mat. Science & Restoration, Proc. Vol., Esslingen 1983.
13. Venečanin S., Influence of Thermal Incompatibility of Concrete Components on Durability of Concrete Pavements (in Serbo-Croatian with summary in English). Proc. Int. Conf. on Modern Achievments in Des., Constr. and Maintenance of Concrete Pavements, Portorož 1985.

Influences of the Arabian Gulf Environment on Concrete Durability

Influences du climat du golfe persique sur la durabilité du béton

Einfluss des Klimas am persischen Golf auf die Dauerhaftigkeit von Beton

Abdul-Hamid J. AL-TAYYIB
Dr. Eng.
Research Institute-KFUPM
Dhahran, Saudi Arabia

Abdul-Hamid J. Al-Tayyib, born in 1946, obtained his Ph. D. in Civil Engineering from Texas Tech. University, Lubbock. At present he is Manager of the Materials and Building Technology Program of the Research Institute at King Fahd University of Petroleum and Minerals.

Abdulaziz I. AL-MANA
Dr. Eng.
Research Institute-KFUPM
Dhahran, Saudi Arabia

Abdulaziz I. Al-Mana, born in 1941, obtained his Ph. D. in Civil Engineering from Stanford University. At present, he is Manager of the Metrology, Standards and Materials Division of the Research Institute at King Fahd University of Petroleum and Minerals (KFUPM).

SUMMARY

In an experimental study, the temperature at various depths of concrete slabs exposed in the field environment of the Arabian Gulf countries has been measured. The effect of the temperature of concrete, which has been found different than that of the ambient air temperature, on its durability has been explained. The surface layer of a deteriorated concrete structure has been chemically analyzed to emphasize the role of air suspended particulate matter in concrete durability.

RÉSUMÉ

Des mesures de température ont été faites à différentes profondeurs d'une dalle en béton exposée aux conditions atmosphériques du golfe persique. L'effet sur la durabilité de la différence de température extérieure et dans le béton est discuté. La couche extérieure d'une structure en béton endommagée a été analysée chimiquement afin de déterminer le rôle des particules suspendues dans l'air.

ZUSAMMENFASSUNG

In einer der Witterung ausgesetzten Betonplatte wurden in verschiedenen Tiefen die Temperaturen gemessen. Die Wirkung der von der Umgebungstemperatur abweichenden Betontemperaturen auf die Dauerhaftigkeit wird besprochen. Die oberste Schicht einer geschädigten Betonstruktur wurde chemisch analysiert, um die Rolle der Luft als Träger suspendierter Stoffe zu belegen.

1. INTRODUCTION

The environmental conditions of the Arabian Gulf region are mainly characterized by its hot summer with virtually no precipitation and high evaporation. The daily mean air temperature in the summer usually varies from 30 to 35^{0}C with maximum temperature as high as 50^{0}C. The mean diurnal swing of air temperature is in the range of 10 to 15^{0}C. The relative humidity varies from 40% to 80%. These environmental conditions of the Arabian Gulf countries are considered to be one of the important factors in the rapid deterioration of concrete structures. Some of the other factors are high salt prevalence in ground, ground water and atmosphere, the scarcity of good quality aggregates, and lack of proper specifications. The deterioration of concrete structures within 10 to 15 years of their service life is common in the Arabian Gulf countries [1]. The various deterioration mechanisms identified in the region are reinforcing steel corrosion, sulfate attack, salt weathering and environmental cracking [2].

In this paper, the results of an experimental study are presented in which the actual temperature of concrete has been measured. Some earlier investigators [3,4] have pointed out that the concrete surfaces may have a temperature 30-40^{0}C higher than that of ambient air temperature. This difference between ambient air temperature and concrete temperature is attributed to the fact that the concrete temperature is not only a function of ambient air temperature, but some other factors also. These include solar radiation, thermal characteristics of concrete, wind speed, heat gain or loss from the ground and the occupied space [5]. If the values reported in the above references [3,4] are assumed, the concrete surface temperature in the Arabian Gulf countries may reach as high as 80-90^{0}C during summer days. Such a high concrete surface temperature coupled with a temperature differential along the depth of concrete may induce significant stresses which may even crack the concrete [6-9].

This study was thought to be important because the available literature provides little experimental data on concrete temperature in the Arabian Gulf countries. Such data is needed in quantifying the environmental stresses and assessing their consequences on concrete durability. The cracking of concrete due to its temperature variations, although usually mentioned in literature, has not been thoroughly investigated. Some studies that have been carried out on this aspect are by Illston and Tajirian [6] and Venecanin [7-9].

Data has also been included in this paper from a separate set of experiments which were carried out to determine the chlorides and sulfates accumulated on the concrete surface from the atmosphere. The objective of this work was to demonstrate that the air suspended particulate matter of the Arabian Gulf environment which contains the deleterious chloride and sulfate salts may play an important role in the durability of concrete even if all the precautionary measures are taken to remove these salts during construction.

2. EXPERIMENTAL PROGRAM

For the measurement of temperature at various depths of concrete, two slabs of dimensions 2 m x 2 m x 0.4 m were cast in the field environment of Dhahran. One slab was cast on a 16 cm thick asphalt-sand composite base which in turn was placed on compacted subgrade soil. While the other slab was cast directly on the compacted subgrade soil. The location of the slabs was such that the sun rays reached the slab surfaces without any obstruction. The slab concrete had 28-day compressive and tensile strengths of 387 kg/cm^2 and 49 kg/cm^2, respectively. Thermocouples were embedded at top, middle and bottom of the concrete slabs at different locations. To facilitate the embedding of the thermocouples, they were first mounted on 10 cm x 10 cm x 40 cm precast beams of concrete similar to that

of slab concrete. The mounted concrete beams were then placed on selected locations and concrete was poured.

In the other set of experiment, which was carried out to realize the role of air suspended particulate matter, the dust accumulated on the surface of a deteriorated concrete structure in Dhahran was collected from different locations using a brush. The dust was then analyzed for chlorides and sulfates.

3. RESULTS AND DISCUSSION

Figures 1 and 2 show the temperature at various depths of concrete slab placed on asphalt-sand base during typical days of summer and winter, respectively. The data on temperature of concrete slab placed directly on subgrade soil is not being presented here due to insignificant difference between the temperature of the two slabs. The maximum difference between the temperature of the two slabs has been found in the range of 0.1 to 2.0 ^{0}C at all the depths.

From Figs. 1 and 2, it can be noticed that the difference between the concrete temperature and ambient air temperature is different for different times of the day and different seasons. During the noon time of summer days, the concrete surface temperature is typically 10 ^{0}C higher than that of the ambient air temperature. However, on few occasions of the one year monitoring period, a difference as high as 15 ^{0}C between the concrete surface temperature and ambient air temperature has been recorded. These differences are low as compared to the ones reported in references [3-5]. However, reasonable agreement has been found between the results of this study and the theoretical study of Illston and Tajirian [6]. The concrete temperature predicted by the computer model of Illston and Tajirian [6] for a concrete slab of dimensions 6 m x 6 m x 0.30 m is shown in Fig. 3 for comparison. Their computer model is based on the following equation:

$$k_s \frac{\partial T}{\partial Z} = -H(T - T_A) + gR - se(\bar{T}^4 - \bar{T}_A^4) \quad ..(1)$$

Where T and $\bar{T}$ are concrete temperatures in ^{0}C and ^{0}K, respectively, T_A and $\bar{T}_A$ are ambient air temperatures in ^{0}C and ^{0}K, respectively, Z is the depth

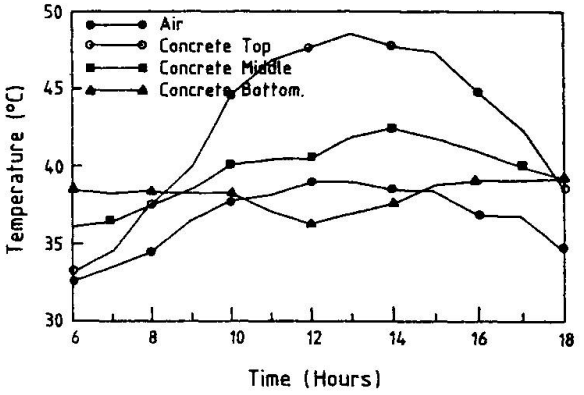

Fig. 1 Variation of ambient air temperature and concrete temperature during a typical summer day in Dhahran

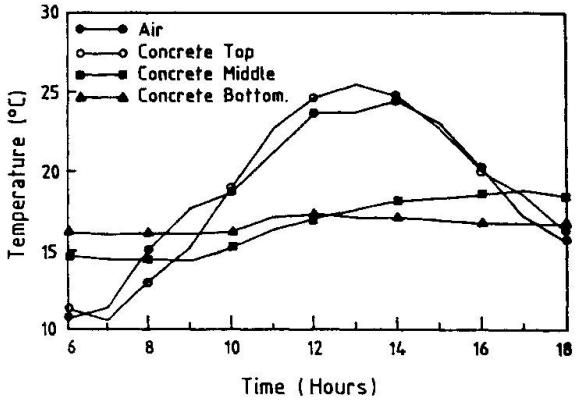

Fig. 2 Variation of ambient air temperature and concrete temperature during a typical winter day in Dhahran

coordinate, k_s is the thermal conductivity of concrete, H is the surface convection factor, g is the absorptivity constant, R is the intensity of solar radiation, s is the Stephan-Boltzmann constant, and e is the emissivity coefficient.

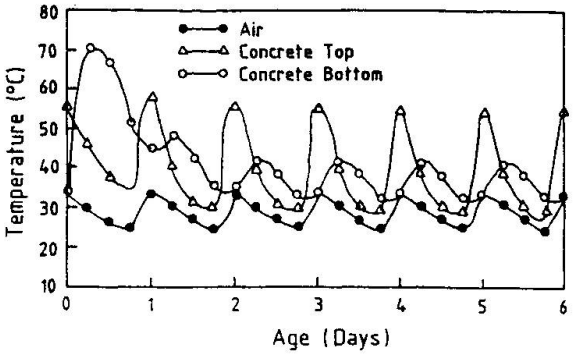

Fig. 3 Concrete temperature predicted by the computer model of Illston and Tajirian (6)

From Fig. 3, it may be noticed that the concrete surface temperature during noon time is approximately 20^0C higher than the ambient air temperature as compared to 10-15^0C in this study. This difference may be attributed to at least two important factors; (a) approximate values of various parameters have been used in equation (1), and (b) the predicted temperatures in Fig. 3 are for a concrete during its first six days of casting when the heat of hydration also contributes in the rise of concrete temperature.

From the results of this study (Figs. 1 and 2), it may also be noted that the typical temperature differential between the top and bottom of slabs during the noon time of summer days is 10^0C, while in winter days it is about 8^0C. During the summer days, temperature differential as high as 15.6^0C has been recorded. The temperature gradient obtained in this study is slightly less than that predicted by Illston and Tajirian [6].

The diurnal change in concrete temperature has been found in the range of 15-20^0C in the summer as well as in the winter. This is higher than the diurnal change in ambient air temperature which is in the range of 10-15^0C.

The large diurnal changes in concrete temperature cause tensile stresses in concrete if the coefficients of thermal expansion of the aggregate and cement paste are significantly different [7-9]. Limestone rock, the commonly available source of coarse aggregates in the Arabian Gulf countries has a coefficient of thermal expansion in the range of 0.9×10^{-6} to $12.2 \times 10^{-6}/^0$C as compared to 10×10^{-6} to $20 \times 10^{-6}/^0$C of hardened cement paste [8]. Venecanin [7] has developed two simple equations that can be used to calculate the stresses in concrete due to daily rise and fall in concrete temperature. These equations include the thermal properties, elastic properties and area of both the aggregate and cement paste along with temperature rise or fall. Considering a coefficient of thermal expansion of $5 \times 10^{-6}/^0$C for aggregates and $15 \times 10^{-6}/^0$C for cement paste along with moderate values of elastic properties and area, tensile stresses that can be generated in the concrete for a temperature change of 15-20^0C are calculated to be 18.75-25.0 kg/cm^2. The magnitude of these type of stresses would decrease with the depth of concrete. As can be seen from Figs. 1 and 2, the diurnal changes in concrete temperature at the middle and bottom of the slab are low as compared to that at the surface. Concrete surfaces subjected to direct sun rays such as airport and road pavements, and bridge slabs are some of the situations where these type of stresses may be significantly high [9].

Another type of stress which may be induced due to temperature is warping stress, particularly in pavement slabs. If there is a large temperature differential along the depth of concrete, the pavement slabs tend to warp and the restraint offered to this warping tendency by the self weight of the slab induces warping stresses. The equations given in reference [10] which are based on Westergaard's analysis and Bradbury's coefficients may be used to calculate such type of stresses. These equations yield a tensile stress of 0.75 kg/cm^2 for the slabs of

this study and for a temperature differential of 15^0C between the top and bottom of the slabs. However, these stresses vary considerably with the dimensions of the slab and its elastic and thermal properties [6]. Keeping the other parameters same, the warping stress in a 5 m x 5 m x 0.4 m slab is calculated to be 13.2 kg/cm^2 as compared to 0.75 kg/cm^2 in the 2 m x 2 m x 0.40 m slab of this study.

The thermal stresses discussed above may not be sufficient to crack a good quality concrete, but in combination with stresses due to loads they may easily do so. Such concrete cracking, which may or may not be structurally dangerous, provides a path for various deleterious salts such as chlorides and sulfates to enter the concrete. These salts initiate or accelerate, if already initiated, the common deteriorating mechanisms, reinforcing steel corrosion and sulfate attack. Even if all the precautionary measures are taken to remove the deleterious salts during the construction phase of concrete, they may come from air suspended particulate matter. This view is supported by the chemical analysis of the surface layer of a deteriorated concrete structure carried out in this study (Table 1). It is believed that the significant amounts of chlorides and sulfates present on the concrete surface are mainly due to high concentration of these salts in the air suspended particulate matter of the Arabian Gulf environment (Table 2).

Location	Cl^- (%)	SO_4^{2-} (%)
1	7.0	21.0
2	8.0	21.0
3	4.5	16.0
4	2.6	18.0
5	5.0	22.0
6	2.0	23.0

Table 1 Chlorides and sulfates on the surface layer of a deteriorated concrete structure in Dhahran

Chemical constituent	Mean concentration ($\mu g/m^3$)		
	Abqaiq	Dhahran	Ras Tanura
Na	13.0	6.0	12.0
K	1.3	1.7	0.9
Ca	21.7	51.8	15.7
Mg	12.7	16.7	7.1
Cl	11.8	18.0	23.2
SO_4	32.6	34.0	23.1
SiO_4	11.9	-	3.9

Table 2 Chemical composition of air suspended particulate matter collected from different parts of Saudi Arabia [reference 11]

4. CONCLUSIONS

This study has revealed that for assessing the influence of temperature on concrete durability, a precise measurement of concrete temperature is necessary. The assessments based on ambient air temperature would be misleading. During the summer days of the Arabian Gulf countries, the concrete surface temperature is 10-15^{0}C higher than that of the ambient air temperature. The diurnal change in concrete temperature is 15-20^{0}C as compared to 10-15^{0}C in ambient air temperature. A temperature gradient as high as 0.4^{0}C/cm has been found along the depth of concrete during summer. In such a temperature regime, significant stresses may be induced in concrete due to thermal incompatibility of concrete constituents. In concrete structures such as pavements, warping stresses may also be present. The thermal stresses in combination with load stresses may easily crack the concrete and once the cracks develop, the chlorides and sulfates

contained in the atmosphere and subsequently settled on concrete surface could enter the concrete and initiate or accelerate the concrete deterioration process.

5. ACKNOWLEDGEMENTS

The authors greatly acknowledge the Research Institute at King Fahd University of Petroleum and Minerals (KFUPM), Dhahran, Saudi Arabia.

6. REFERENCES

1. AL-TAYYIB, A.J. and KHAN, M.S., Concrete Deterioration Problems in the Arabian Gulf- A Review. Durability of Building Materials, Vol. 4, 1987, pp. 287-298.

2. RASHEEDUZZAFAR, DAKHIL, F.H. and Al-GAHTANI, A.S., Deterioration of Concrete Structures in the Environment of the Middle East. ACI Journal, Vol. 81, No. 1, 1984, pp. 13-20.

3. MIRONOV, S.A., MALINSKYI, E.N. and VAKHITOV, M.M., Durability Assessment Criterion for Concrete Exposed to Dry Hot Climatic Conditions. Durability of Building Materials, Vol. 1, 1982, pp. 3-14.

4. DE SERIO, J.N., Designing for Effects of Creep, Shrinkage, Temperature in Concrete Structures. Special Publication SP-27, American Concrete Institute, Detroit, Michigan, 1971, pp. 43-49.

5. ASHTON, H.E. and SEREDA, P.J., Environment, Microenvironment and Durability of Building Materials. Durability of Building Materials, Vol. 1, 1982, pp. 49-65.

6. ILLSTON, J.E. and TAJIRIAN, A., Computer Experiments on Environmentally Induced Stresses in Unreinforced Concrete Pavement Slabs. Magazine of Concrete Research, Vol. 29, No. 101, 1977, pp. 175-190.

7. VENECANIN, S.D., Durability of Concrete Materials as Influenced by Different Coefficients of Thermal Expansion of Components. Durability of Building Materials and Components, ASTM STP 691, P.J. Sereda and G.G. Litvan, Eds., American Society for Testing and Materials, 1980, pp. 179-192.

8. VENECANIN, S.D., Influence of Temperature on Deterioration of Concrete in the Middle East. Concrete, Vol. 11, No. 8, 1977, pp. 31-32.

9. VENECANIN, S.D., Influence of Thermal Incompatibility of Concrete Components on Durability. The Arabian Journal for Science and Engineering, Vol. 11, No. 2, 1986, pp. 157-166.

10. YODER, E.J. and WITCZAK, M.W., Principles of Pavement Design. John Wiley and Sons, New York, Second Edition, 1975, pp. 85-88.

11. Sampling and Characterization of Ambient Air Suspended Particulate Matter in Abqaiq, Dhahran and Ras Tanura. Report, Water Resources and Environment Division, Research Institute, King Fahd University of Petroleum and Minerals, Dhahran, Saudi Arabia, March 1983, 55 pp.

Removal of Concrete by Acidic Water

Usure du béton par de l'eau acide

Betonabtrag durch saure Wässer

Horst GRUBE
Dr.-Ing.
Forschungsinst. Zementindustrie
Düsseldorf, BR Deutschland

Horst Grube, geboren 1938, promovierte als Bauingenieur an der TH Darmstadt. Er leitete 12 Jahre das zentrale Baustofflabor einer Grossbaufirma und ist seit 8 Jahren stellv. Leiter der Hauptabteilung Betontechnik im Forschungsinstitut. Arbeitsschwerpunkte: Ausführung und Dauerhaftigkeit von Betonbauwerken, Durchlässigkeit gegenüber Flüssigkeiten und Gasen, Kriechen, Schwinden, Instandsetzung.

Wolfram RECHENBERG
Dr.-Ing.
Forschungsinst. Zementindustrie
Düsseldorf, BR Deutschland

Wolfram Rechenberg, geboren 1931, promovierte als Chemiker an der TU Hannover. Er war 5 Jahre als Entwickler für Gummiasbest und Klebebänder tätig. Seit 22 Jahren ist er wissenschaftlicher Mitarbeiter des Forschungsinstituts und betreut die chemische Analyse. Zu seinen Aufgabengebieten gehört der chemische Angriff auf Beton und die Erfassung von Zementwerksemissionen.

SUMMARY

The attack of acidic water must be assessed when planning durable concrete structures. The aggressiveness is generally expressed in terms of concentration of attacking acid. A protective layer built up by reaction products and its stability can have a much greater influence on the loss of material than the concentration of the attacking substances. Experiments, based on a calculation model, show how to estimate the loss of material (the amount of affected concrete) to be expected under practical conditions. Parameters are the type and the concentration of the acid solution, the composition of the concrete and the stability of the protective layer.

RÉSUMÉ

Il faut tenir compte de l'attaque possible des eaux acides lors de projet de structures en béton durables. Le degré d'attaque est en général donné par la concentration de l'acide. Une couche protectrice formée par des produits de réaction et sa stabilité peuvent avoir une influence plus importante sur le taux d'usure que la concentration de la solution attaquante. Des expériences basées sur un modèle de calcul montrent comment estimer le taux d'usure dans les conditions réelles de construction. Les paramètres sont le genre et la concentration de la solution d'acide attaquant, la composition du béton et la stabilité de la couche protectrice.

ZUSAMMENFASSUNG

Der Angriff saurer Wässer muss bei der Planung dauerhafter Betonbauwerke berücksichtigt werden. Der Angriffsgrad wird im allgemeinen durch die Konzentration der angreifenden Säure angegeben. Eine aus Reaktionsprodukten gebildete ungestörte Schutzschicht kann einen wesentlich grösseren Einfluss auf die Abtragsrate haben als die Konzentration der angreifenden Lösung. Versuche auf der Grundlage eines Rechenmodells zeigen, wie man die Abtragsrate unter baupraktischen Bedingungen abschätzen kann. Einflussgrössen sind Art und Konzentration der angreifenden sauren Lösung, die Zusammensetzung des Betons und die Stabilität der Schutzschicht.

1. INTRODUCTION

Water which contains diluted acid, e.g. lime-attacking carbonic acid, will affect concrete. The acid dissolves the calcium from its bonds. As a result, the concrete is progressively destroyed from the surface to the inside. The rate at which the hardened cement paste and possibly the aggregate are dissolved mainly depends on the concentration of the attacking acid in the water and on the chmical resistance of the concrete. Many standards determine the degree of attack primarily on the basis of the concentration of the aggressive substances, e.g. ISO standard /1/. Test results show /2,3,6/ that only a very small proportion of the aggressive substances in the running water reacts with the hardened cement paste. Beyond that the chemical resistance of the concrete against a solvent attack can be enhanced by using insoluble aggregates and cement with a higher SiO_2 content /4,5/ and by keeping the water cement ratio low ($w/c < 0{,}60$). The flow rate seems to have very little influence /7/ as long as we stay within the ground water range of flow rates. This behaviour is to be explained by the formation of a protective layer of SiO_2 gel which, with increasing duration of attack, acts as a barrier to the transport of aggressive substance to and removal of dissolved constituents from the concrete. The chemical resistance of the concrete against solvent attacks is thus essentially depending on the existence of that protective layer. Reference to these correlations was made by several authors /8-11/. However, in planning and designing concrete structures they are not yet generally considered. It was therefore the objective of our study to develop a mathematical model for estimating in advance the loss of concrete as a function of the concrete composition, the concentration of the aggressive solution and the stability of the protective layer.

2. COURSE OF REACTION

Tests have shown /11,12/ that carbon dioxide (CO_2) dissolved in water first leads to the formation of a thin layer of calcium carbonate ($CaCO_3$) in the areas of mortar or concrete which are close to the surface. Then additional CO_2 dissolves the $CaCO_3$ to form $Ca(HCO_3)_2$ which is removed by the water. Next in the same process calcium from the calcium silicates is dissolved and removed. What remains is a gel-like layer consisting of hydrous silicon dioxide which also contains iron and aluminium oxide /11,13/. The gel layer becomes thicker with progressing attack. If a solid material forms a protective layer, the rate of dissolution will become essentially independent of the flow rate of the solution. In that case it will only be determined by the thickness and the diffusion resistance of the protective layer. This dissolution process can be slowed down further by reducing the flow rate of the surrounding water towards zero and by increasing the diffusion resistance in the environment of the concrete by a tight soil.

3. DETERMINING THE CaO REMOVAL FROM MORTAR AND CONCRETE

Koelliker measured the rate at which CaO is removed by dissolution from 4 x 4 x 16 cm^3 Portland cement mortar prisms containing about 500 kg of cement per cubic meter and having a water-cement ratio of 0.50 /11,12/. Lime-dissolving carbonic acid was dissolved in the attacking water. The resulting pH value was about 4.4. The surface-related rate of dissolution decreased (following approx. a $1/\sqrt{t}$ law) with increasing exposure time. This indicates that, due to the effect of the lime-dissolving carbonic acid, a protective layer forms which gains in thickness in the course of time and thus increasingly blocks the diffusion of the dissolved CaO.

By means of a model based on Fick's first law equation 1 was developed /14/ which can be used for calculating the thickness d of the destroyed layer after any given exposure time t. The influencing variables are the diffusion coefficient, the mass of soluble matter per volume unit, the area percent of the soluble matter in the area of attack and the difference in $Ca(HCO_3)_2$ concentration:

$$d = \sqrt{\frac{2 \quad D \quad A_l}{m_l \quad A_{ges}} (c_s^* - c_l)} \cdot \sqrt{t} \qquad /1/$$

whereby

d	is the thickness of destroyed concrete layer in cm
D	$Ca(HCO_3)_2$ diffusion coefficient in cm^2/s of the protective layer (gel layer) ($D \approx 1.8 \cdot 10^{-6}$ $cm^2 \cdot s^{-1}$ for SiO_2 gel of hardened Portland cement paste)
m	mass of soluble matter in g of CaO per cm^3 of concrete
c_s^*	CaO-concentration in g/cm^3 in the $Ca(HCO_3)_2$-solution surrounding intact concrete
c_l	CaO-concentration in g/cm^3 in the $Ca(HCO_3)_2$-solution which is unaffected by the concrete
A_l/A_{ges}	ratio of soluble matter area to total area in the cross section
V_l/V_{ges}	ratio of the volume of soluble constituents (if insoluble aggregate is used volume of hardened cement paste) to total volume

$A_l/A_{ges} = V_l/V_{ges}$

Examples of computation including the determination of the concentration difference $(c_s^* - c_l)$ are given in /14/.

The first root in equation 1 represents a constant valid in the respective case. Equation 1 can therefore be simplified to form equation 2.

$$d = a \cdot \sqrt{t} \qquad /2/$$

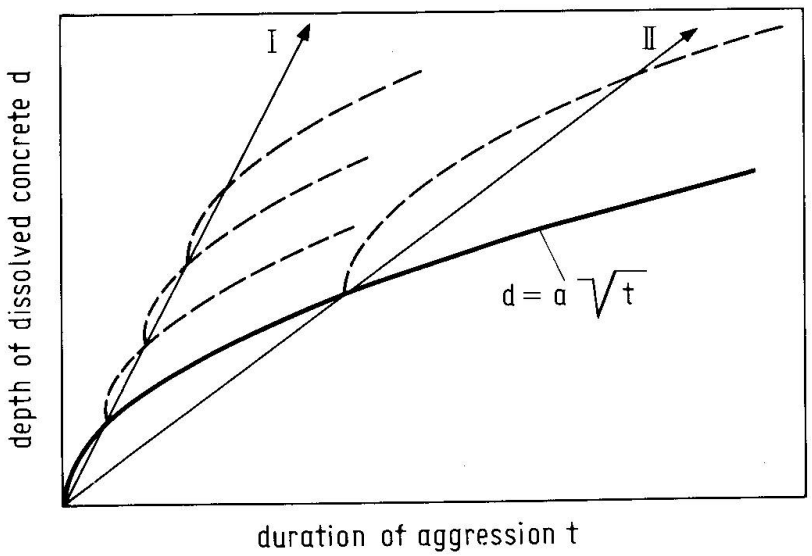

Fig. 1 Acceleration of a solvent attack when removing the protective layer periodically

The loss of mass which occurs with an intact protective layer and follows equation 2 is shown by the full bold line in Fig. 1. It had been assumed earlier that the loss of mass might follow a $\sqrt{t}$ law /6, 8-10/. However, in the past it was not possible to describe different test periods by one function. This was due to the fact that the test specimens were dabbed with a moist cloth before being weighed. In this way part of the gel-like protective layer was removed so that the subsequent reaction occurred much faster than it would have done with an intact protective layer. If the protective layer is removed

regularly it is to be expected that the parabolic function turns to a linear one as shown by the straight lines I and II in Fig. 1. The "linear loss of mass" will be the steeper the more frequently the protective layer is removed (straight line I). It will be the flatter the less frequently the protective layer is removed (straight line II). This "linear loss of mass" has already been observed in connection with long-term tests /3/.

In order to verify this behaviour experimentally 4 x 4 x 16 cm prisms according to DIN 1164 were made with a 35 F Portland cement and a 35 L blast furnace slag cement. They contained 550 kg/m^3 of cement and had a water-cement ratio of 0.50.

The prisms were produced and stored in water by the standard procedure. At the age of 7 days they were placed in tap water which was continuously enriched with CO_2 and renewed every week. The lime-attacking carbonic acid content was about 110 mg CO_2/l, the pH was 6.15 (mean values). The water flow rate was about 4.2 10^{-2} cm/s. The experimental setup is described in detail in /2/.

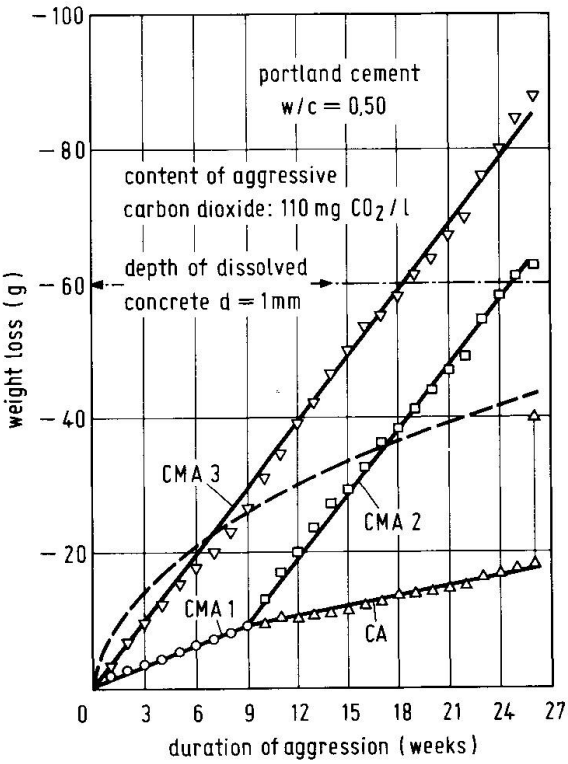

Fig. 2 Weight loss of PC-mortar prisms by aggressive carbon dioxide. Different intervals for removing the protective layer

The results for Portland cement mortar in Fig. 2 show that the weight loss resulting from the uniform chemical attack by 110 mg CO_2/l depends very much on the type and intensity of the additional mechanical treatment. In an initial series of tests the prisms were only dabbed once a week (CMA 1 in Fig. 2). After nine weeks some of the prisms were brushed once a week (CMA 2), the others were not subjected to any further mechanical treatment (CA). The prisms of the second test series were brushed three times per day throughout the test period (CMA 3).

The storage without any further mechanical treatment describes the chemical attack in slowly running water according to ISO DP 9690 /1/ with the diffusion being controlled by the protective layer. Dabbing presents a mild and brushing a vigorous additional mechanical treatment (M) of the protective layer.

The rate of concrete removal for CMA 3 was approx. 1 mm in 18 weeks or about 3 mm/a in the 4 x 4 x 16 cm prisms (a weight loss of 60 g corresponds to about 1 mm of loss of concrete). The rate of concrete loss was lower for the blast furnace slag cement mortars /14/ than it was for the Portland cement mortars. This leads to the assumption that the higher content of silicon oxide and the resulting lower content of calcium oxide in blast furnace slag cement might be an explanation for this behaviour. The question, however, was not studied in greater detail.

The various losses of mass obtained in the tests are below the ones calculated using equation for, e.g., weekly losses, because brushing did not remove all of the SiO_2-gel from the pores. The longer the time period of an undistur-

bed gel layer was the better was the agreement between the calculated and the experimental results /14/. This can be seen from the dotted line in Figure 2, which shows the calculated depth of dissolved concrete according to equation 1. The first brush off at the age of 26 weeks shows the marked value slightly below the calculated value.

4. PRACTICAL APPLICATION

In addition to the construction cost the design engineer should include in his considerations the service life and the repair and maintenance cost of a structure. If concrete is exposed to acids the resulting loss of mass may be irrelevant to its use. This often is the case for structures like foundations or drilled foundation piles. In contrast, the practical use of a container or a water duct where the protective layer may be removed regularly can be considerably impaired by a constant loss of e.g. 0.5 mm of concrete per year. Therefore the design engineer, besides considering the acid concentration in the attacking water, should also pay attention to the external conditions on which the concrete is exposed to the water. For illustration Fig.3 shows the depth of concrete loss in mm after 20 years for different conditions of transport and different content of aggressive CO_2. The conditions of transport are described in Table 1.

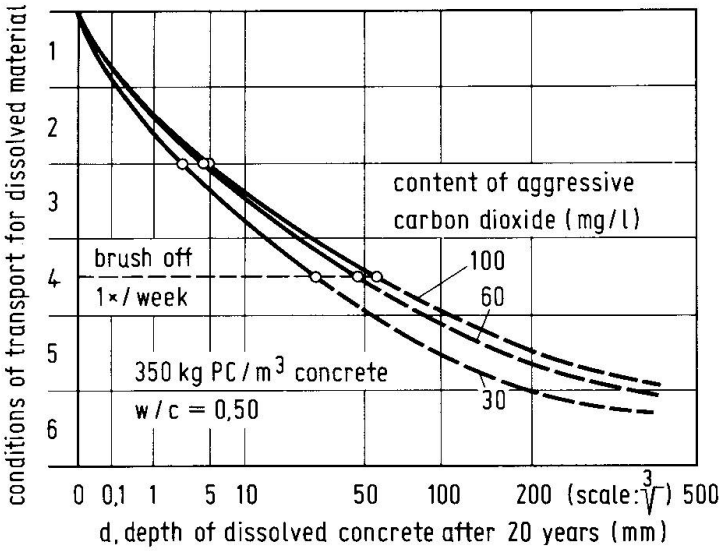

Fig. 3: Depth of dissolved (and removed) concrete after 20 years in different concentration of aggressive carbon dioxide at different conditions of transport (see below) for the products of the reaction

The dots in the figure represent the results of experiments and calculations. The dotted parts of the curves in the areas of TC 5 and 6 are extrapolations that can at present not be validated by test results.

CT 1	Compact deposited soil, permeability $k < 10^{-4}$ cm/s, very slowly moving or stagnant ground water, protective layer, Fick's 2. law.
CT 2	Permeable soil with $k \geq 10^{-4}$ cm/s, ground water moving slowly, protective layer, Fick's 1. law.
CT 3	Flowing free water, protective layer nearly undisturbed, Fick's 1. law
CT 4	Flowing free water, protective layer removed periodically, Fick's 1. law
CT 5	Flowing free water, high velocity of flow, no protective layer, approximation to specific velocity of dissolution.
CT 6	Flowing free water, very high velocity of turbulent flow, cavitation.

Table 1 Conditions of transport (CT) according to Fig. 3

5. CONCLUSIONS

- The diffusion model presented here and the tests described permit to arrive

at a quantitative estimate of the loss of mortar and concrete to be expected in case of a chemical attack by lime-dissolving carbonic acid.

- The exposure to lime-dissolving carbonic acid leads to the formation of a protective layer consisting of gel-like silicon dioxide.

- In the presence of an intact protective layer the loss of mass (the amount of affected concrete) follows a $\sqrt{t}$ law.

- If the protective layer is mechanically destroyed the concrete is removed at an accelerated rate.

- A disturbance of the protective layer, even if it occurs at relatively long intervals, can have a much more damaging effect than an increase in the concentration of the aggressive acid.

- The tests described, i.e. the stripping of the protective layer at regular intervals, and the mathematical model permit a long-term estimate of the loss of mass also caused by other than lime-dissolving carbonic acid. Experiments with other acids can be made in about 3 months.

- It appears possible to consider more completely in future standards the factors which reduce and increase the loss of mass from concrete exposed to attacking acids. This would be to the benefit of concrete structures. It is suggested to define the degrees of attack by solved mass or the affected depth of concrete respectively.

6. REFERENCES

1. ISO-Draft DP 9690 (1987): Classification of environmental exposure conditions for concrete and reinforced concrete structures. ISO-TC 71/SC3.
2. Locher, F.W., und S. Sprung: Die Beständigkeit von Beton gegenüber kalklösender Kohlensäure. beton 25 (1975) H. 7, S. 241/245.
3. Locher, F.W., W. Rechenberg und S. Sprung: Beton nach 20jähriger Einwirkung von kalklösender Kohlensäure. beton 34 (1984) H. 5, S. 193/198.
4. Friede, H., P. Schubert und H.P. Lühr: Angriff kalklösender Kohlensäure auf Beton. beton 29 (1979) H. 7, S. 250/253.
5. Efes, Y., und H.P. Lühr: Beurteilung des Kohlensäure-Angriffs auf Mörtel aus Zementen mit verschiedenem Klinker-Hüttensand-Verhältnis. TIZ-Fachberichte 104 (1980) H. 3, S. 153/167.
6. Friede, H.: Zur Beurteilung des Angriffs kalklösender Kohlensäure auf Beton. Dissertation RWTH Aachen 1983.
7. Gille, F: Über den Einfluß des Kalkgehalts des Zements und des Zuschlags auf das Verhalten des Betons in sauren Wässern. beton 12 (1962) H. 10, S. 467/470.
8. Tremper, B.: The Effect of Acid Waters on Concrete. Journal of the Amer. Concr. Inst., Proc. 28 (1932), S. 1/32.
9. Rombèn, L.: Aspects of Testing Methods for Acid Attack on Concrete. CBI forskning research 1:78 und 9:79, Cement- och betong institutet, Stockholm.
10. Polak, A.F.: Mathematical Model of Concrete Corrosion in Acidic Media. Beton; Zhelezobeton, Nr. 8, (1978), S. 5/6.
11. Koelliker, E.: Über die Wirkung von Wasser und wäßriger Kohlensäure auf Beton. Intern. Kolloquium "Werkstoffwissenschaften und Bausanierung", Berichtsband TA Esslingen, 1983, S. 195/200. E. Moeller GmbH, Filderstadt.
12. Koelliker, E.: Cem. Concr. Res. 15, 100 (1965).
13. Grün, R., und K. Obenauer: Einwirkung von Kohlensäure auf Zementmörtel und Beton. Zement 33 (1944) H. 1, S. 10/12.
14. Grube, H., und W. Rechenberg: Betonabtrag durch chemisch angreifende saure Wässer. beton 37 (1987) H. 11, S. 446/451, und H. 12, S. 495/498.